PHILOSOPHICAL TRANSACTIONS OF THE ROYAL SOCIETY A MATHEMATICAL, PHYSICAL & ENGINEERING SCIENCES

The Thermodynamics of the Titanium + Oxygen System: An Isothermal Gravimetric Study of the Composition Range Ti$_{3}$O$_{5}$ to TiO$_{2}$ at 1304 K

R. R. Merritt and B. G. Hyde

Phil. Trans. R. Soc. Lond. A 1973 **274**, 627-661
doi: 10.1098/rsta.1973.0078

THE THERMODYNAMICS OF THE TITANIUM+OXYGEN SYSTEM: AN ISOTHERMAL GRAVIMETRIC STUDY OF THE COMPOSITION RANGE Ti_3O_5 TO TiO_2 AT 1304 K

BY R. R. MERRITT† AND B. G. HYDE

AND, IN PART (SECTION 7),

L. A. BURSILL AND D. K. PHILP

School of Chemistry, University of Western Australia, Nedlands, W.A. 6009, Australia

(*Communicated by J. S. Anderson, F.R.S. – Received 2 February* 1973)

[Plate 8]

CONTENTS

† Present address: C.S.I.R.O., Division of Mineral Chemistry, P.O. Box 124, Port Melbourne, Victoria, 3207, Australia.

 [Published 9 August 1973

The compositions of titanium oxide samples at 1304 K have been studied by, as far as possible, equilibrating them with (H_2+H_2O) gas buffer mixtures of various compositions. The high precision with which the mass, and therefore the sample's composition, was determined reveals that complete equilibrium is rarely attained, even after several days in a constant ambient: at most compositions there is gross hysteresis.

Two composite hysteresis loops exist in the regions occupied by the (121) and (132) crystallographic shear structure families. Between these loops the oxidation and reduction paths are very nearly coincident: this is the region in which a change in composition can be accommodated by varying only the orientation and not the number of crystallographic shear planes. A third hysteresis loop is believed to exist between the (132) loop and the composition of slightly reduced rutile. A plausible explanation of the behaviour is developed. All the observations appear to be consistent with those from parallel electron microscope studies of reduced 'rutile'. Nucleation of the product phase appears to be the most important factor affecting the behaviour in the region Ti_3O_5 to Ti_4O_7, as would be expected from a consideration of their structures.

The differences between the behaviour observed by us and that reported by other workers is believed to be only apparent: it results from (*a*) the higher precision of our measurements, and (*b*) the much higher density and number of data points we have acquired.

Various thermodynamic data are calculated for the many higher titanium oxides on the basis of a reasonable assumption for deducing approximate *equilibrium* oxygen potentials from the observed values. Most of these have not previously been available. By incorporating Zador's (1967) data for $TiO_{1.99}$ to $TiO_{1.999}$ we deduce for $\frac{1}{3}Ti_3O_5+\frac{1}{6}O_2 = TiO_2$ (rutile), $\Delta G^{\ominus}$ (1304 K) $= -78.3$ kJ mol^{-1} compared with -79.4 kJ mol^{-1} in the JANAF tables. The stabilities of the Ti_nO_{2n-1} phases with respect to mixtures of the $(n-1)$ and $(n+1)$ neighbours are seen to be extremely small (-10_4 J/mol of Ti_7O_{13}, i.e. -5.2 J/mol of atoms), and to decrease with increasing n.

1. Introduction

A knowledge of both thermodynamics and structure is essential for understanding inorganic solids, particularly those that exhibit non-stoichiometry. During the last 20 years there has been a considerable increase in structural knowledge and understanding (Wadsley 1964), but thermodynamics has not kept pace. The experimental techniques have not generally matched those for studying structure, in precision or incisiveness. The lag is a serious handicap. In solid phase transformations structure is an important factor and indeed it may strongly affect the observed thermodynamics, as Ubbelohde (1956) has convincingly demonstrated. But, quantitatively, the driving force for a solid state reaction is most conveniently measured in thermodynamic terms, and so reaction mechanisms and kinetics may be said to depend on or at least reflect thermodynamic properties. Thermodynamic measurements can also provide a simple, direct way of detecting structurally related effects, such as the strain energy in reacting crystals, which may radically alter the rates of diffusion and other processes.

Quantitative theories of non-stoichiometry and the 'defect solid state' lead most directly to thermodynamic conclusions, and these are amenable to experimental testing. In cases of slight non-stoichiometry theory and fact appear to be consistent (Kröger 1964), but for wide variations in composition this is not so. The structural model for most statistical thermodynamic treatments involves complete disorder (see, for example, Wagner & Schottky 1930), whereas structural studies have often revealed substantially complete order, with 'homologous series' of closely related structures. Of particular interest are those series of phases whose structures are derived from a simple parent structure by crystallographic shear (c.s.).

The titanium oxides are most significant: their compositions vary almost continuously (at least in some ranges) from Ti to TiO_2. Structurally they are at least as well described and understood as any multiphase binary system, and so they seemed an obvious 'test case' for a detailed study in order to attempt a reconciliation of thermodynamics and structure, especially the higher oxides ($x = O/Ti \geqslant 1.7500$) which are all c.s. structures. The thermodynamic data already available in the literature are not entirely consistent with the structural observations. Furthermore, either they are not very comprehensive, or their quality is not very impressive: insufficient data and poor precision leave their interpretation open to speculation, in a field where, as we shall see, speculation has proved to be insufficiently reliable or fertile.

In what follows we restrict ourselves to the titanium oxides from Ti_3O_5 to TiO_2. The available thermodynamic and structural information is reviewed in § 2. In § 3 we justify our choice of experimental technique, and describe our apparatus and experimental procedure. The results are described in § 4, and analysed in largely phenomenological terms in § 5. Derived thermodynamic quantities are presented in § 6, and a structural interpretation of the observed behaviour is given in § 7. This involves an assessment of the information now available from electron microscopy/diffraction studies; it reveals a new 'solid solution' phenomenon that allows thermodynamic bivariance even in a completely ordered crystal of variable composition.

2. Previous knowledge of the titanium oxides TiO_x, $1.75 \lesssim x < 2.00$

(a) *Phase and structure analysis*

The structural key came from investigations by the Swedish school (Andersson, Collén, Kuylenstierna & Magnéli 1957; Andersson 1960; Andersson & Jahnberg 1963). X-ray diffraction studies revealed an archetypal example of the resolution of apparently homogeneous non-stoichiometric phase regions into a homologous series of ordered structures. Phases Ti_nO_{2n-1} with integral values of $n = 4$ to 9 had structures derived from the TiO_2 (rutile) type by regular crystallographic shear on (121) planes.† X-ray diffraction methods could not resolve the structures and phase relations at higher compositions ($x \geqslant 1.90$), but subsequent electron microscope/diffraction studies uncovered a wealth of detail. Slightly reduced rutile contains a maze of disordered c.s. planes parallel to {132} (Eikum & Smallman 1965; Bursill, Hyde, Terasaki & Watanabe 1969; Bursill & Hyde 1970; Anderson & Tilley 1970). Further reduction leads to their aggregation (Bursill & Hyde 1971 *a*) and ordering to give a series of structures, analogous to the earlier series but with (132) c.s. planes (Bursill *et al.* 1969; Bursill & Hyde 1971 *b*). These occupy the composition range $1.93 \lesssim x \lesssim 1.98$, and also have stoichiometries Ti_nO_{2n-1}, but apparently only with even values of n. (These observations are consistent with the suggestions

† All indices refer to a rutile type cell or subcell.

of Anderson & Hyde (1967), but were not available when the work to be described here was started.) The observed n values are temperature-dependent, changing from $16 \leqslant n \lesssim 40$ at about 1300 K to $12 \leqslant n \lesssim 40$ at 1673 K.

(*b*) *Thermodynamics*

Previous thermodynamic studies have been quite numerous, but often their aim has been simply to elucidate the nature of slightly reduced rutile, $1.99 \lesssim x < 2.00$: in fact, less than that, to try to distinguish between alternative defect models for accommodating the oxygen deficit in $TiO_{2-\delta}$, i.e. interstitial titanium atoms/ions or vacant oxygen sites. The gravimetric measurements of Kofstad (1962), Førland (1964), and Moser, Blumenthal & Whitmore (1965) are concordant. They were interpreted as indicating the presence of ionized anion vacancies. But the logical basis of this approach is always weak and for $TiO_{2-\delta}$ it is completely unsound, since the possibility of random c.s. planes was not even considered.

The solid state cell measurements of Blumenthal & Whitmore (1963) and Zador (1967, 1969) extend down to $x \approx 1.96$, and suggest a lower homogeneity limit of $x \approx 1.99$ for $TiO_{2-\delta}$ (at 1273 K), with a diphasic region at lower compositions.

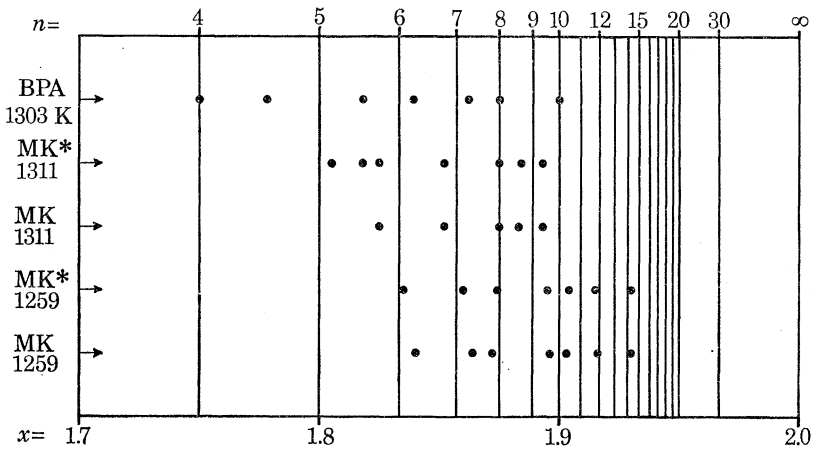

FIGURE 1. Stationary compositions observed by Bogdanova, Pirogovskaya & Ariya (1963), and Morozova & Konopel'ko (1965). The vertical lines occur at the ideal stoichiometries Ti_nO_{2n-1}. The values BPA and MK are those reported by the authors concerned; the values MK* were deduced by the present authors from the published isotherms of Morozova & Konopel'ko.

Bogdanova, Pirogovskaya & Ariya (1963) studied lower compositions, and concluded that their results conflicted with the structural data of Andersson *et al.* (1957); but Hyde & Eyring (1965*a*) pointed out that this need not be so. The *stationary compositions* (x independent of oxygen activity) were in fairly good agreement with the ideal crystallographic stoichiometries for $n = 4$, 8 and 10, and in fair agreement for $n = 6$ and 7 (figure 1). But they also occurred at $n \approx 4\frac{1}{2}$ and $5\frac{1}{2}$, and Hyde & Eyring suggested that these might indicate members of a series $Ti_{n'}O_{2n'-2}$ with $n' = 9$ and 11 or, alternatively, *pseudo-phases* (diphasic solids exhibiting bivariance; Hyde, Bevan & Eyring 1966) with compositions at half-integral n values only by chance. Morozova & Konopel'ko (1965) obtained isotherms similar to that of Bogdanova *et al.* but their interpretation resembled that of Hyde & Eyring. It invoked the possibility of *continuity* (Ubbelohde 1956) in the phase reactions, and metastable states. This should cause hysteresis, but the experimental data were ambiguous on this point.

In both cases data points were sparse; there were some discrepancies between the measured compositions and those expected from the ideal formula Ti_nO_{2n-1} (cf. figure 1), and the reproducibility of these stationary compositions was not very good. The compositional accuracy appeared to be $\delta x \lesssim 0.007$, which is rather poor when $\Delta x/\Delta n = 0.014$ for $n = 8$ going to $n = 9$, and even less for higher n.† It is especially limiting in the interesting region $x \gtrsim 1.900$ where, at that time, the only available experimental data of any sort were those of Morozova & Konopel'ko (1965) at 1259 K, which tended to support the suggestion of Andersson & Jahnberg (1963) that higher oxides ($n > 9$) probably existed.

For the following reasons it seemed important that the Russian work be repeated, but with a higher accuracy and many more data points.

(i) Their measurements had not unequivocally confirmed the crystallographically determined compositions of Andersson's phases.

(ii) The behaviour in the region $x \gtrsim 1.90$ might reveal the existence of new ordered phases and their stoichiometries.

(iii) The existence of hysteresis in the phase reactions was suspected but not tested. (Hysteresis is an important but not widely appreciated aspect of the thermodynamic behaviour of real, as distinct from model, non-stoichiometric crystals.)

After our experiments were finished two further papers were published. Vasil'eva & Shaulova (1969) used a solid state electrochemical cell to measure the partial molar free energy of oxygen in three samples at 1100 to 1300 K. Their compositions corresponded to the phase mixtures ($Ti_3O_5 + Ti_4O_7$), ($Ti_6O_{11} + Ti_7O_{13}$) and ($Ti_8O_{15} + Ti_9O_{17}$). Anderson & Khan (1970) published the results previously referred to (Anderson 1970): their conclusions were similar to those of Bogdanova *et al.* and Morozova & Konopel'ko, but again the data were sparse and the compositional accuracy was not very high: ± 0.0025 in x.

(*c*) *Conclusions*

The higher titanium oxides provide a beautiful, complex, and structurally fairly well-delineated example of multiple c.s. structures. They are thermodynamically accessible. (The oxygen activities are neither too high nor too low.) Except at very high temperatures (Gilles 1970) their study is not complicated by the problem of evaporation of the solid (which makes thermodynamic studies of, for example, WO_x and MoO_x so difficult). Earlier thermodynamic work on the systems Pr + O (Hyde *et al.* 1966) and Tb + O (Hyde & Eyring 1965*b*) had indicated that the true thermodynamic behaviour of a complex system might only be revealed clearly if a very high density of data points were obtained. All measurements, but particularly that of the solid's composition, must be more accurate than had been achieved in previous studies.

It was also clear that the structural features should be defined as thoroughly as possible. Hence, simultaneous structural and thermodynamic investigations were started. The outcome confirms our belief that this dual approach to a single system is more powerful than either taken separately.

The thermodynamic data reported here still do not provide a complete picture. Subsequent structural studies (cf. § 2*a* above), and the interpretation of the present data have revealed the need for further measurements, especially at high temperatures. These are commencing, but the data already available allow a considerable advance in our understanding of the behaviour of this system and, by inference, others.

† For example, Morozova & Konopel'ko ascribed the observed $TiO_{1.893}$ at 1311 K to $Ti_{10}O_{19} = TiO_{1.900}$' but the higher $TiO_{1.896}$ at 1259 K to $Ti_9O_{17} = TiO_{1.889}$.

3. Experimental techniques

(a) *Choice of a method*

Of the several methods available for studying partial molar free energies in solids such as titanium oxides which have variable composition and low oxygen activities, monitoring the very high temperature evaporation process by mass spectrometry (e.g. Gilles 1970) is insufficiently precise for our purpose. Two precision methods are in common use. One employs a solid state electrochemical cell (e.g. Zador 1967) in which the oxide under investigation forms one electrode, separated from a reference electrode by a solid electrolyte in which the transport number of oxygen ions is very close to unity. If the partial molar free energy of oxygen $[G_m(O_2)]$ in the reference electrode is known, that in the sample can be determined by measuring the cell e.m.f.

$$E = [G_m(O_2, \text{sample}) - G_m(O_2, \text{reference})]/4F.$$

The composition of the sample can be changed by coulometric titration, i.e. transferring oxygen between the electrodes by means of an impressed e.m.f. Composition changes are then determined by applying Faraday's laws. In the other method the solid is equilibrated with a gas buffer mixture of known composition, usually $H_2 + H_2O$ or $CO + CO_2$, for which the partial molar free energy of oxygen is known. The sample is suspended from a balance so that changes in its composition are readily monitored. The precision with which $G_m(O_2)$ can be determined is about the same for the two methods: approx. $0.5\,\text{mV} \equiv 0.2\,\text{kJ}\,(\text{mol}\,O_2)^{-1}$. But there are important differences, and these will now be discussed.

(i) Coulometric titration may lead to problems associated with irreversibility, particularly when the system being studied exhibits hysteresis, as in the present case. The impressed e.m.f. needed to 'drive' the titration at a reasonable rate may be quite high. (Fender & Riley (1970) give about $0.1\,\text{V} \equiv 40\,\text{kJ}\,(\text{mol}\,O_2)^{-1}$.) Only a part of this will be dropped across the sample, but a high resistance specimen is likely to be considerably polarized. In gravimetric experiments the increments in $G_m(O_2)$ may be very small, and severe gradients thus avoided. (In our experiments they were often as little as $0.2\,\text{kJ}\,\text{mol}^{-1} \equiv 0.5\,\text{mV}$.) It is therefore obvious that the progress of $G_m(O_2)$ during an oxidation or reduction run is monotonic in a gravimetric experiment, but must be oscillatory when coulometric titration is used.

(ii) In principle it is perhaps easier to measure composition changes to a high precision by coulometric titration ($\delta x \approx \pm 2 \times 10^{-5}$) than by gravimetry ($\delta x \approx \pm 2 \times 10^{-4}$, corresponding to $\delta m \approx \pm 20\,\mu\text{g}$, in our experiments).† However, there are uncertainties in coulometric titration which are absent from gravimetry. Obviously the former assumes $t(O^{2-})$ is exactly unity. Even if this is so at close to equilibrium it may not be when a relatively high external e.m.f. is applied. More important, there must be only *electrochemical* transfer of oxygen, i.e. no chance that oxygen be transported through the ambient gas or vacuum either during coulometric titrations *or at any other time*. Transporting agents such as hydrocarbons (from pump oil), hydrogen, water, oxides of carbon, etc. (and, of course, oxygen) must be rigorously excluded. As well as causing compositional errors this sort of transport (or even the possibility of it occurring) may cause difficulty in interpreting the behaviour of the cell. (An example of this occurs in Zador (1967), and is discussed in § 5 *d* (iv).)

† With extreme care a better accuracy may be achieved: $\delta m \approx \pm 1\,\mu\text{g}$, or $\delta x \approx \pm 1 \times 10^{-5}$; cf. Felmlee, Hyde & Randall (1972).

(iii) Finally, the composition (mass) of the sample can be monitored continuously in gravimetric experiments, though not in cell measurements. Especially in view of the uncertainty implied by (ii), this is a considerable advantage.

Thus, both methods have their merits but, for present purposes, we believe the advantage lies with the gravimetric method, which we therefore used.

(*b*) *Apparatus and procedure*

Figure 2 is a schematic diagram of the apparatus. A gas buffer mixture ($H_2 + H_2O$) was circulated in a closed system containing a 0.5 g sample of titanium oxide suspended from a *Cahn RG* recording, vacuum balance *l*. The oxide was in a Pt + 3 % Rh bucket *n* at the thermal centre of a non-inductively wound tube furnace *p*, 0.6 m long, the temperature of which was controlled to ± 1 K. The water vapour pressure was controlled by a water-containing cryostat *i* in the circulating system. The gas flow rate was sufficiently high (0.7 to 1.4 m s^{-1} down the inner tube *x*, 0.07 to 0.14 m s^{-1} up the outer annulus $q - x$) to prevent significant thermal segregation. This was confirmed by varying the flow rate and observing that the mass remained constant when conditions were set so that the sample's composition was very sensitive to a change in the composition of the gas buffer.

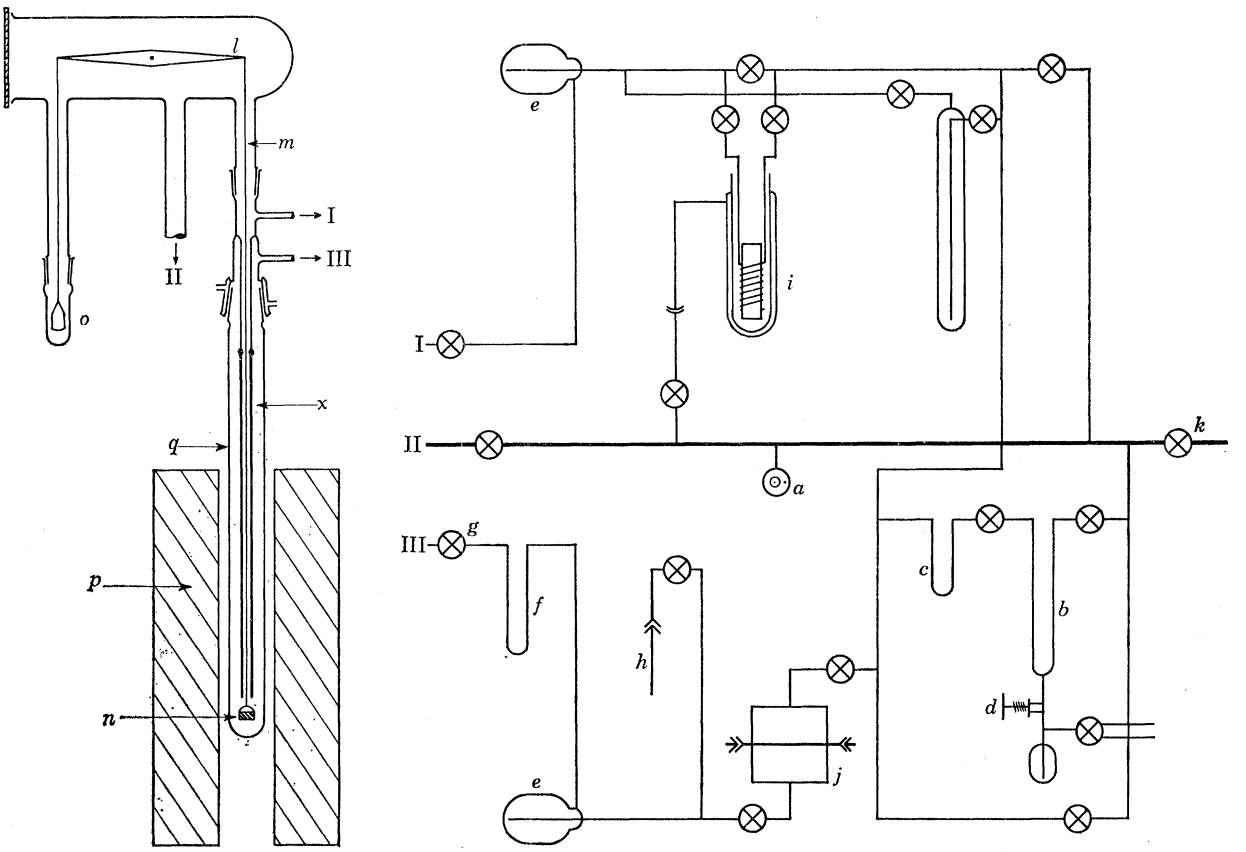

FIGURE 2. Schematic diagram of (on the right) the gas circulating system and (on the left) the balance and sample section of the apparatus. *a*, ionization gauge; *b*, mercury manometer; *c*, silver foil trap; *d*, diaphragm valve; *e*, 5 dm^3 ballast volumes; *f*, flow meter; *g*, throttle valve; *h*, storage vessel for degassed water; *i*, cryostat; *j*, gas circulating pump; *k*, tap to cold trap and vacuum pumps; *l*, balance; *m*, 0.1 mm diameter hangdown wire (Pt + 13% Rh); *n*, sample bucket (Pt + 3% Rh); *o*, counterpoise weights; *p*, furnace; *q*, quartz hangdown tube; *x*, alumina inner tube.

All the measurements were made with a sample temperature of 1302 to 1305 K, the mean value being 1304 K. After determining the reference mass (as $x = 2.0000$; see (*c*) below) the system was evacuated, and an experiment was started in one of two ways, depending on whether it was to start with reduction of TiO_2 or oxidation of Ti_3O_5. (For the region $1.75 \leqslant x \lesssim 1.98$ there are possibly relevant structural factors, cf. § 5*b*.)

In the first, water vapour was admitted to a pressure of 1.3 kPa (10 Torr), and then hydrogen to a total pressure of 6.7 to 13.3 kPa (50 to 100 Torr). Water often condensed in the system at this stage. This mixture was then circulated for about 50 ks† during which the sample lost mass, *some of which was regained* as a final steady composition was approached. The starting sample was therefore produced by oxidation; and its transpires that this is important, cf. § 5*d*. The run then consisted of controlled reduction in steps achieved by small hydrogen increments, or decrements in the cryostat temperature, followed by controlled oxidation.

In the second the starting sample was Ti_3O_5 or a $Ti_3O_5 + Ti_4O_7$ mixture. This was produced by reducing rutile with 'dry hydrogen', i.e. hydrogen circulated via a trap cooled in liquid air, instead of through the cryostat. Once the desired starting composition was attained the trap was replaced by the cryostat, and controlled incremental oxidation commenced.

The gas flow affected the apparent sample mass. Hence, at 600 s intervals, the circulating pump *j* (Arnold *et al.* 1969) was automatically switched off for 46 s. This allowed time for the gas flow to decay and the sample's mass to be recorded, but without a significant mass change due to thermal segregation.

Starting materials were rutile powder or single crystal; typical analyses are given in table 1. The gases were (*a*) water, from de-ionized water that had been thoroughly degassed by repeated freezing, pumping and thawing before being transferred by evaporation from a reservoir *h* into the cryostat *i*; and (*b*) high purity (cylinder) hydrogen manufactured by diffusion through palladium.

TABLE 1. SPECTROGRAPHIC ANALYSES OF RUTILE SAMPLES

	powder		
element	before use	after use	single crystal
Cr	< 0.002 %	< 0.002 %	0.05 to 0.2 %
Al	< 0.002	< 0.002	0.002
Fe	< 0.002	< 0.002	0.05 to 0.2
Ni	n/a	n/a	0.05
Pt	not found	< 0.05	n/a
Rh	not found	< 0.05	n/a
Cu	—	—	< 0.002
Mg	—	—	< 0.002
Ca	—	—	< 0.002

The sample mass and temperature and the cryostat temperature were simultaneously and continuously logged by a multipoint recorder (0.3 % accuracy). The total gas pressure was measured with a wide (17.5 mm) precision bore mercury manometer *b* and a cathetometer. The water-vapour pressure was deduced from the recorded cryostat temperature. (A preliminary experiment determined the relation between these: 23 points in the range $0.2 \lesssim p(H_2O) \lesssim 1.3$ kPa (1.5 to 10.0 Torr) were used to derive a 'best fit' polynomial. The values were slightly higher than those in the literature (Weast 1966), but by no more than 6.6 Pa (0.05 Torr), i.e. little more

† 1 h = 3.6 ks; 1 day = 86.4 ks; 1 week = 0.6048 Ms.

than the inaccuracy in measuring the pressure. The discrepancy is probably due to a small difference between the effective temperature of the cryostat and that at the junction of the thermocouple used to measure it. Vapour pressures lower than the measured values, and down to 13 Pa (0.10 Torr), were deduced by extrapolating the same fourth degree polynomial.)

(*c*) *Accuracy and precision*

To resolve by gravimetry the highest oxides (revealed by electron diffraction) a high precision in measuring the sample's composition is essential. Equally, their unambiguous identification demands a high accuracy. (Attainment of a pure monophasic solid is also necessary.) Phases Ti_nO_{2n-1} exist, at least up to $n \approx 36$ and, since $x = O/Ti = (2n-1)/n = 2-(1/n)$, it follows that $dx/dn = 1/n^2$ and hence $\Delta x/\Delta n \approx 0.0008$ at $n = 36$. Adjacent (132) c.s. phases probably differ by $\Delta n = 2$, in which case $\Delta x \approx 0.0015$ at $n = 36$. A precision/accuracy of $\delta x \gtrsim \pm 0.0005$ would therefore seem to be needed.

TABLE 2. ESTIMATED MAXIMUM UNCERTAINTIES AND PRECISION OF THE MEASUREMENTS

parameter	uncertainty	precision
sample temperature/K	±4	±1
partial molar free energy of oxygen/kJ mol^{-1}	2.5 to 4.8†	0.20 to 0.28
sample composition, x in TiO_x	0.002 to 0.003‡	0.0002 (≡ 20 μg)

† Made up of approx. 2.4 kJ mol^{-1} from uncertainty in the sample temperature, 1 kJ mol^{-1} from uncertainty in $\Delta G^{\ominus}$ for the reaction $H_2(g)+\frac{1}{2}O_2(g) = H_2O(g)$ (Wagman *et al.* 1945), 1 kJ mol^{-1} from uncertainty in the calibration of $p(H_2O)$ as a function of the cryostat temperature, 0.2 kJ mol^{-1} from uncertainty in the cryostat temperature, and 0.005 kJ mol^{-1} from uncertainty in the pressure of the gas buffer mixture.

‡ But see text, this page.

Generous estimates of uncertainties in the recorded experimental data are combined to yield the accuracies and precisions listed in table 2. As the work progressed it became clear that, in fact, the accuracy in measuring the sample composition was very much better than estimated. Stationary compositions were observed over wide ranges of oxygen activity at $TiO_{1.7499}$ and $TiO_{1.6664}$; compositions which are expected to be ideally

$$TiO_{1.7500} = Ti_4O_7 \quad \text{and} \quad TiO_{1.6666} = Ti_3O_5.$$

The main source of uncertainty here is in determining a reproducible reference mass at a known composition (e.g. to correct for zero drift in the balance). The design of the *Cahn* balance made this something of a problem. Finally, we used $TiO_{2.0000}$ as the assumed reference composition of a sample of oxide at 1304 K in pure oxygen at a pressure of 1.33 to 2.66 kPa (10 to 20 Torr). Corrections for the effect of gas pressure, which with a *Cahn RG* are not simply buoyancy effects (T. L. Felmlee & B. G. Hyde 1969, unpublished work), were obtained from previous calibrations of apparent mass *vs.* gas pressure in oxygen and in various gas buffer mixtures, using the normal experimental arrangement with only the oxide sample missing. Again, we believe that this procedure is justified by the experimentally determined compositions of Ti_3O_5 and Ti_4O_7. Several determinations of the reference mass indicate a compositional *accuracy* of $\delta x \approx 0.0002$.

4. Experimental results

In our experience a systematic thermodynamic study of a complex system like TiO_x must be preceded by exploratory experiments which yield a general understanding of the gross features of its behaviour. From this one can plan the procedure for a detailed investigation. In (*a*) we describe these broader aspects; in (*b*) the more systematic and detailed experiments.

(*a*) *The broad pattern of behaviour revealed by preliminary experiments*

(i) *Effect of temperature on kinetics; Si contamination*

Experiments at 1343 and 1303 K revealed that reaction rates were about the same at both temperatures. The lower was therefore selected for the runs as this would (*a*) facilitate a comparison of our results with those of Bogdanova *et al.* (1963) and Morozova & Konopel'ko (1965), and (*b*) reduce the possibility of contaminating the sample with Si from SiO (g). From the data of Kubaschewski, Evans & Alcock (1967) we calculate $p(\mathrm{SiO}) = 0.1\,\mathrm{mPa}$ to $0.3\,\mu\mathrm{Pa}$ (10^{-9} to $10^{-11.5}$ atm) at 1304 K for our range of gas buffer ratios. The corresponding values from data in the JANAF tables (Stull 1965) are higher: 1.6 mPa to 10 μPa ($10^{-7.8}$ to 10^{-10} atm). The chance of Si contamination is actually less than these figures would suggest because the circulating gas approaches the sample via the *alumina* inner tube (*x* in figure 2). Any SiO (g) would be formed after this, and swept up the outer annulus to the cold part of the outer quartz tube *q*. And the gas flow rate is very high. Nevertheless, runs were expected to be prolonged (up to several months), and so it was important to keep $p(\mathrm{SiO})$ as low as possible.

(ii) *Approach to equilibrium*

Oxygen transfer between solid and gas was usually very slow, but markedly slower for $x < 1.88$ than for higher compositions. After changing the buffer ratio the sample's mass almost always 'drifted' for a considerable time: usually it would still be changing at an appreciable rate 130 ks (36 h) later. Hence it was necessary to compromise between getting a large number of data points at non-steady masses and a few data points at close to a *steady mass* condition. [A steady mass is defined as a rate of not more than $0.55\,\mathrm{ng\,s^{-1}}$ ($2\,\mu\mathrm{g\,h^{-1}}$), corresponding to the sample's composition changing at $\dot{x} \ngtr 5.5\,\mathrm{Gs^{-1}}$ (0.00002 per hour, 0.0005 per day, 0.003$\dot{3}$ per week).†]

A steady mass criterion for 'equilibrium' depends on (*a*) the precision in measuring the composition and/or (*b*) one's patience. Both Bogdanova *et al.* and Morozova & Konopel'ko had used a quartz helix balance which, for a 0.5 g sample capacity would have a precision of approx. 150 μg. The former claimed that 'equilibrium was reached in 3 to 4 h for the reduction of the specimen and in an appreciably longer time for its oxidation'. In contrast, Morozova & Konopel'ko said that their 'experiments were run continuously for 30 to 40 hours.... We assumed equilibrium obtained when the mass of oxide remained constant for 12 to 15 h': which corresponds to a steady mass criterion of about 7.0 to $5.6\,\mathrm{ng\,s^{-1}}$ or $\dot{x} \approx 60\,\mathrm{Gs^{-1}}$. Our steady masses are certainly 'equilibrium' values by this criterion, and so are most of our other masses that were clearly still changing. Anderson & Khan (1970) state that 'non-equilibrium' is a problem at 1273 K, but not at higher temperatures, $T \geqslant 1323$ K. They do not, however, discuss their criterion for 'equilibrium'.

Neither a fixed time interval after setting new ambient conditions nor a fixed rate of change of

† It will be appreciated that even much larger rates are still very slow, so that even quite small changes of composition would require extremely long times; i.e. complete equilibration is quite impracticable.

mass appear to provide suitable criteria for 'approximate equilibrium' in the Ti + O system. Therefore, in addition to sample temperature and composition and the (relative) partial molar free energy of oxygen, $\Delta G_m(O_2)$,† in the gas atmosphere over the sample, at each datum point in the systematic runs we also recorded the rate of change of the sample's composition (usually averaged over the final 5.4 to 7.2 ks, and normally $\dot{x} < 100\,\mathrm{Gs}^{-1}$), and the time elapsed since the ambient conditions had been established. This last was 3.6 to > 36 ks and, it should also be emphasized, the increments in $\Delta G_m(O_2)$ were very small, cf. (iii).

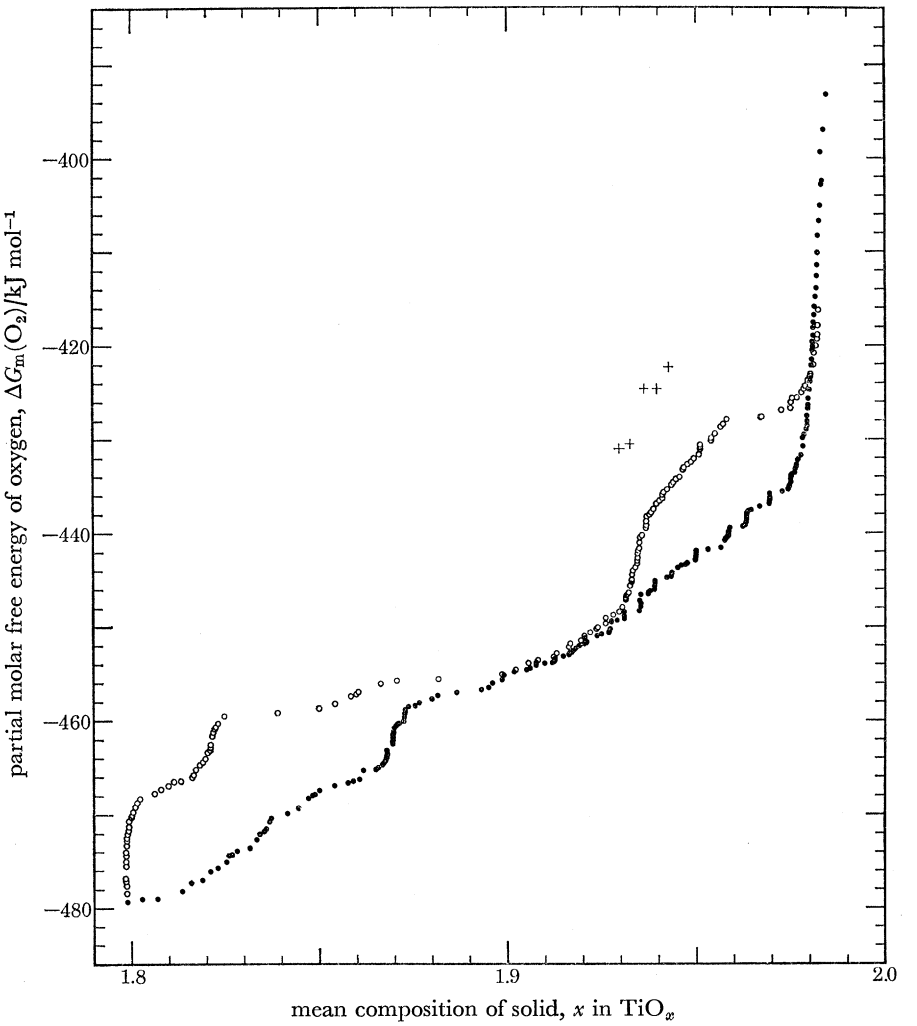

FIGURE 3. Run 4: the isotherm for controlled reduction from $TiO_{1.9846}$ to $TiO_{1.7990}$ (●), and oxidation to $TiO_{1.9825}$ (○). The points + are from the data of Golubenko & Rezukhina (1967), extrapolated a little to 1304 K.

(iii) *Density of data points*

Resolution of the higher homologues Ti_nO_{2n-1} with $n > 15$ requires a large number of very closely spaced data points, and so increments in $\Delta G_m(O_2)$ had to be small: not more than 200 to 400 J mol^{-1}. (About 1000 recorded points are used in this paper; too many to tabulate.)

† $\Delta G_m(O_2) = G_m(O_2) - G^\circ_m(O_2) = RT \ln a(O_2)$, the reference state being oxygen gas with a fugacity of 101 325 Pa = 1 atm, at T = 1304 K.

(iv) *Reversibility*

When the progress of an experiment was reversed (from oxidation to reduction or vice versa) a steady mass was usually maintained (or attained very rapidly) at the next few points. Often the mass remained constant, or nearly so, over a range $\Delta[\Delta G_m(O_2)] \approx 5$ to 10 kJ mol^{-1} (cf. § 7*a*.)

(v) *Effect of varying the preliminary preparation of the sample*

If the conditions for the preliminary reduction of the rutile sample (the first procedure in § 3*b*) were changed so that the starting composition was rather less than $x \approx 1.981$ the subsequent reaction rates were much lower, and variations in the slope of the isotherm much less pronounced (cf. § 4*b* below).

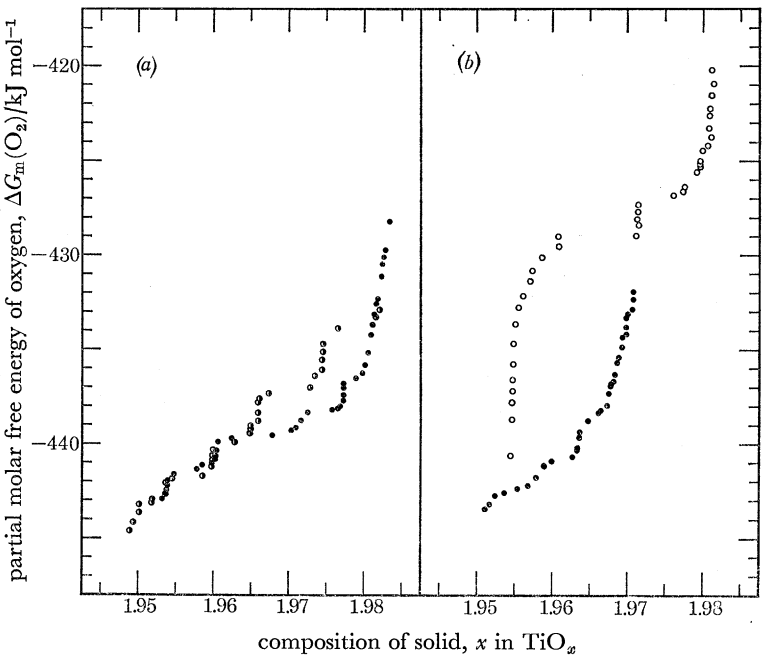

FIGURE 4. (*a*) Isotherms for runs 1 (●), and 2 (◑); reduction only. (*b*) Isotherm from run 3: reduction from $TiO_{1.9708}$ to $TiO_{1.9511}$ (●) was followed by oxidation to $TiO_{1.9812}$ (○). Note that the obvious 'steps' in (*a*) are absent in (*b*); the result of too great a preliminary reduction. The oxidation leg in (*b*) is obviously a scanning curve inside a hysteresis loop.

(*b*) *Systematic runs*

The longest uninterrupted run lasted two months, and covered the composition range down to $x = 1.7990$: run 4, the data for which are reproduced in figure 3. A sample of $TiO_{1.9846}$, prepared as described in § 3*b*, was reduced in small steps (205 data points) and then reoxidized (142 points) to $TiO_{1.9825}$.

Runs 1 and 2 started similarly, but ended prematurely and accidentally. They consisted of reduction legs only: $1.9821 \geqslant x \geqslant 1.9489$ and $1.9834 \geqslant x \geqslant 1.9532$ (figure 4*a*).† The data from run 3 (figure 4*b*) are in strong contrast, and show the effect of too great a preliminary reduction (cf. § 4*a*(v)): steady masses were only very slowly achieved. Starting at $x = 1.9708$ the sample was incrementally reduced to $x = 1.9511$, and then reoxidized in steps to $x = 1.9812$.

These first four runs used rutile powder. Run 6 used a few single crystal rutile chips. They were

† For clarity, not all the available data points are plotted in figures 4 to 7.

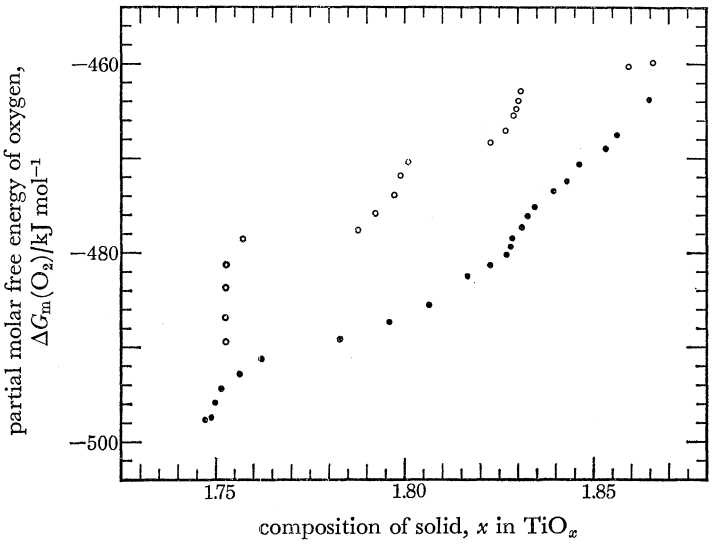

FIGURE 5. Run 6, using a few single crystal chips. The sample was first reduced in dried hydrogen and then incrementally oxidized (○), from $TiO_{1.753}$ to $TiO_{1.866}$, and reduced (●) to $TiO_{1.747}$. Note the narrow ranges of almost stationary composition.

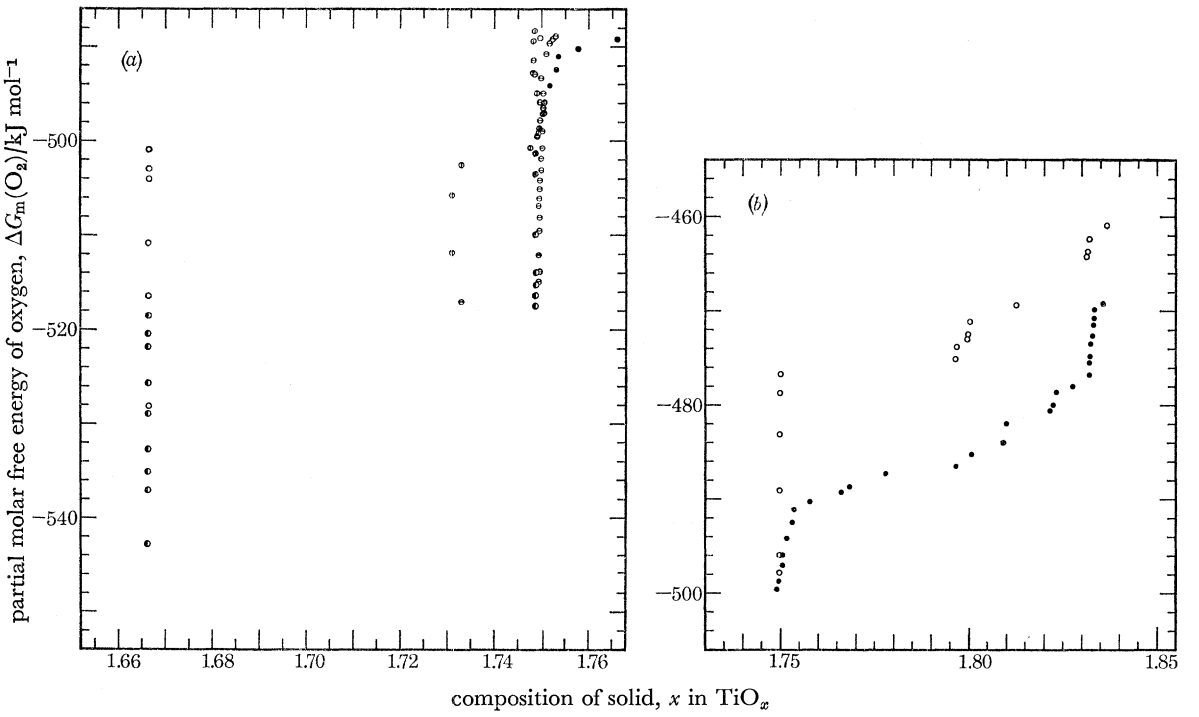

FIGURE 6. Run 8: single crystal rutile was reduced to $x \approx 1.73$ using dried hydrogen, and then oxidized to $x = 1.773_6$. It was then incrementally reduced (⊖) to $x = 1.731$, oxidized (⊕) to $x = 1.749_5$, reduced (◐) to $x = 1.666_3$, oxidized (○) to $x = 1.836_7$, and finally reduced (●) to $x = 1.748_7$. (*a*) shows the region Ti_3O_5 to Ti_4O_7, (*b*) the region Ti_4O_7 to just above Ti_6O_{11}. Note the two line phases in (*a*) and, in (*b*), the clear indications of Ti_4O_7, Ti_5O_9 and, especially in reduction, Ti_6O_{11}.

first reduced with 'dry' hydrogen (§ 3*b*). When the cryostat was substituted for the liquid air trap the mass of the sample increased rapidly until the mean composition was $\bar{x} = 1.753$. It was then oxidized to $x = 1.866$, and then reduced to $x = 1.747$. The data (figure 5) are within 0.84 kJ mol^{-1} of those from a similar run with a powder sample.

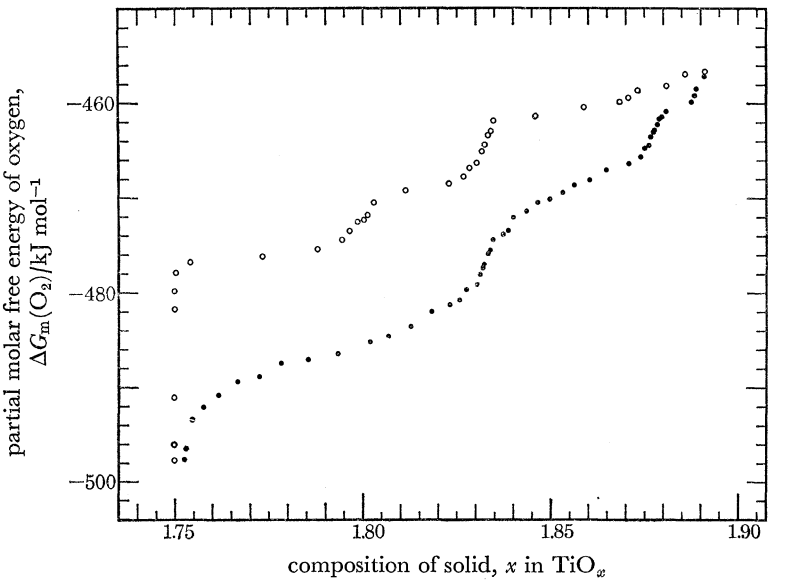

FIGURE 7. Run 9: a repeat examination of the region $1.75 \leqslant x \leqslant 1.89$ starting with Ti_3O_5 prepared from single crystal rutile, but with ice + salt as cryostat coolant instead of the CO_2 (s) + propanol used in run 8. Again note the comparatively clear indications of Ti_nO_{2n-1} with $n = 4$, 5, 6 and 8 and, possibly, 9. ○, oxidation; ●, reduction.

For run 8 the cryostat coolant was changed from the normal ice + salt to solid CO_2 + propanol, so that lower oxygen potentials could be achieved and the region Ti_3O_5 to Ti_4O_7 examined. (Using ice + salt it was not possible to reduce the sample beyond $x \approx 1.75$.) It started with the reduction of a rutile single crystal by 'dry' hydrogen to a composition $x \approx 1.73$. The sample was then oxidized directly to $x = 1.7736$. In the first part of the run it was reduced in increments to $x = 1.731$, and then reoxidized in steps to $x = 1.7495$. It was then reduced again in increments to $x = 1.6663$ at the minimum accessible $\Delta G_m(O_2) = -542.8$ kJ mol^{-1}, and then reoxidized in steps to $x = 1.836_7$. Finally, it was reduced in steps to $x = 1.748_7$. The data are shown in figures 6*a* and *b*. In this run a problem arose at higher compositions: because of the quite large difference between the temperatures of the water reservoir and the coolant in the cryostat, relatively large fluctuations in the cryostat temperature occurred (up to about 0.2 or 0.3 K).

To obviate these, in run 9 a rutile single crystal was first reduced to Ti_3O_5 by using a high $p(H_2)/p(H_2O)$ buffer ratio: the ratio was then reduced so that the sample oxidized to a mean composition $\bar{x} = 1.71$. At this point the cryostat was isolated, and the dry ice + isopropanol coolant replaced by ice + salt. When the cryostat was again cold it was reconnected into the gas circulating system, the sample reoxidizing rapidly to $x = 1.75$. This product was then incrementally oxidized to $x = 1.8912$ and reduced to $x = 1.7525$. The data are plotted in figure 7. Where they overlap, these two runs yielded data in very good agreement.

5. Discussion and partial interpretation of the data

Runs 4 and 8 overlap in the region $1.7990 \leqslant x \leqslant 1.8367$ (figures 3 and 6*b*). Taken together they show that a single hysteresis loop extends from $x = 1.75$ to $x \approx 1.90$. In run 4 it was truncated by changing from reduction to oxidation at $x = 1.7990$; in run 8 conversely at $x = 1.8367$. This loop was almost completely circumnavigated in run 9 (figure 7).

Taking this into account, runs 4 and 8 together provide a good overall view of the behaviour of the system over the whole composition range from $TiO_{\sim 1.67}$ to $TiO_{\sim 1.98}$. The data fall naturally into five composition regions with the boundaries at $x \approx 1.75$, 1.90, 1.93 and 1.98. In the lowest no *stationary compositions* (x independent of $\Delta G_m(O_2)$) were observed between the limiting values $TiO_{1.66}$ and $TiO_{1.75}$. In the third and fifth ($1.90 \lesssim x \lesssim 1.93$ and $x \gtrsim 1.98$) the oxidation and reduction paths are almost coincident, but not quite so. In the second and fourth ($1.75 \lesssim x \lesssim 1.90$; $1.93 \lesssim x \lesssim 1.98$) this is by no means the case; gross hysteresis obtains.

At this stage the most readily understood behaviour occurs in the lowest range and so we will discuss it first; and then the others in order of increasing difficulty. A completely new type of phenomenon exists in the region $1.90 \lesssim x \lesssim 1.93$ between the hysteresis loops: but a comprehensive discussion demands not only some very recently acquired structural data (Bursill, Hyde & Philp 1971), but also the equilibrium thermodynamic properties derived in § 6. A full discussion, which also throws light on the possible cause of the excessive hysteresis in the two loops, is therefore postponed to § 7.

(*a*) *The region* $1.66 \leqslant x \leqslant 1.75$

The facts appear to be straightforward here.

(i) Two highly reproducible stationary compositions (with steady masses) were observed at $x = (1.6664 \pm 0.0001)$ and $x = (1.7499 \pm 0.0002)$, each over a wide range of oxygen potentials. These presumably correspond to the crystallographically defined phases Ti_3O_5 and Ti_4O_7. They show no detectable homogeneity range.

(ii) Similar phenomena were observed when the oxygen potential was increased over Ti_3O_5 or reduced over Ti_4O_7: no composition change occurred until a critical ratio $p(H_2)/p(H_2O)$ was attained, and then only after an induction period of about 7.2 ks.† Then, during the next 5.4 ks the mass changed at a rate which increased, at first slowly and then rapidly, to a maximum $|\dot{x}| = (0.55 \pm 0.08)\ \mathrm{Ms}^{-1}$. This rate was maintained across what is clearly the diphasic $Ti_3O_5 + Ti_4O_7$ region, dropping abruptly when the composition of the product phase was reached. These observations suggest that there is a large nucleation barrier to the oxidation of Ti_3O_5 and the reduction of Ti_4O_7 (cf. the values of $\Delta G_m(O_2)$ in figure 6*a*). Once it is surmounted reaction continues until the conversion is complete, without any change in oxygen potential being necessary. The partial molar free energy of oxygen when Ti_4O_7 started to reduce was

$$517.04 > -\Delta G_m(O_2) > 514.96\ \mathrm{kJ\,mol^{-1}} \quad \text{(experiment 1)},$$

$$518.52 > -\Delta G_m(O_2) > 517.46\ \mathrm{kJ\,mol^{-1}} \quad \text{(experiment 2)}.$$

When Ti_3O_5 started to oxidize it was

$$500.88 > -\Delta G_m(O_2) > 497.83\ \mathrm{kJ\,mol^{-1}}.$$

Thus the 'irreversibility' is about $17\ \mathrm{kJ\,mol^{-1}}$.

† Each buffer ratio was maintained for 7.2 to 43 ks before it was changed.

(iii) Another experiment was designed to reduce this gap of 17 kJ mol^{-1}, mainly to determine more accurately the standard free energy change for the phase reaction

$$Ti_3O_5(s) + O_2(g) = Ti_4O_7(s).$$

The reduction of Ti_4O_7 was interrupted at $x = 1.705$ by increasing $p(H_2O)/p(H_2)$ until the reaction stopped. It was then raised in small steps until oxidation started. No reaction was detectable ($|\dot{x}| \gtrsim 5.5\,Gs^{-1}$) in the range $512.12 \geqslant -\Delta G_m(O_2) \geqslant 508.36$ kJ mol^{-1}, an interval of 3.76 kJ mol^{-1}. The sample was then reduced to Ti_3O_5, reoxidized to $x = 1.705$, and $\Delta G_m(O_2)$ values noted for stopping the oxidation, starting reduction, stopping reduction and recommencing oxidation. In this case the range was $510.87 \geqslant -\Delta G_m(O_2) \geqslant 506.68$ kJ mol^{-1}, an interval of 4.19 kJ mol^{-1}. Even here there may be some 'irreversibility'; a maximum of

$$512.12 - 506.68 = 5.44\,kJ\,mol^{-1},$$

and a minimum of $508.36 - 510.87 = -2.51$ kJ mol^{-1}. There appears to be a hysteresis loop which, at $x = 1.705$, is approx. 5.44 kJ mol^{-1} wide. When the reactions are reversed the scanning curves overlap by about 2.51 kJ mol^{-1}. Perhaps the proposed 'nucleation barrier' is too simple an explanation.

The Ti_3O_5 structure (Åsbrink & Magnéli 1959) is certainly topologically different from that of Ti_4O_7: the oxygen arrays are distorted c.c.p. and h.c.p. respectively. A reconstructive

$$Ti_3O_5 \rightleftharpoons Ti_4O_7$$

transformation, in the sense used by Buerger (1951), therefore seems reasonable. However, this glosses over the structural details of the transformation which recent work (Iwasaki, Bright & Rowland 1969) suggests may be more complex than is implied by the adjective 'reconstructive'. It is conceivable that there are polymorphs of Ti_4O_7 and, especially, Ti_3O_5† based on each type of oxygen array. It is perhaps possible that one of the latter, isostructural with V_3O_5, may exist as a metastable intermediate in the reduction of Ti_4O_7. (Since this work was completed we have discovered that the existence of Ti_3O_5 with the V_3O_5-type structure *has* been reported (Åsbrink *et al.* 1971).)

(*b*) *The region* $1.75 \leqslant x \lesssim 1.90$

The *equilibrium* thermodynamic behaviour of an isothermal binary system with a sequence of independent, solid, 'line' phases is depicted schematically in figure 8*a*. In this region the observations are radically different.

Hysteresis is commonly observed if the phases are closely related in structure especially if, as in the present case, the differences in stoichiometry are small. Adjacent phases may then occur coherently or semi-coherently. They will not be independent, and the appropriate phase rule will be $F > C - P + 2$. In Ubbelohde's (1956) terms, phase reactions will be *continuous*, and *hybrid* crystals will occur.

In the rare earth oxide systems PrO_x (Hyde *et al.* 1966) and TbO_x (Hyde & Eyring 1965*b*) one observes a series of monophasic, highly ordered solids, with simple hysteresis loops at intervening compositions. This situation, shown schematically in figure 8*b*, is again not what we observe here with TiO_x. Instead there appears to be a composite loop resulting from the fusion or overlapping of several individual loops, such as occur separately in figure 8*b*. This coincides with the composition range of the Andersson phases Ti_nO_{2n-1} with $4 \leqslant n \lesssim 10$, i.e. $1.75 \leqslant x \lesssim 1.90$.

† In this connexion it may be germane that, in the similar series of vanadium oxides V_nO_{2n-1}, V_3O_5 *is* a member of the (121) family of rutile-derived c.s. structures with $n = 3$; a fact that seems to have escaped notice.

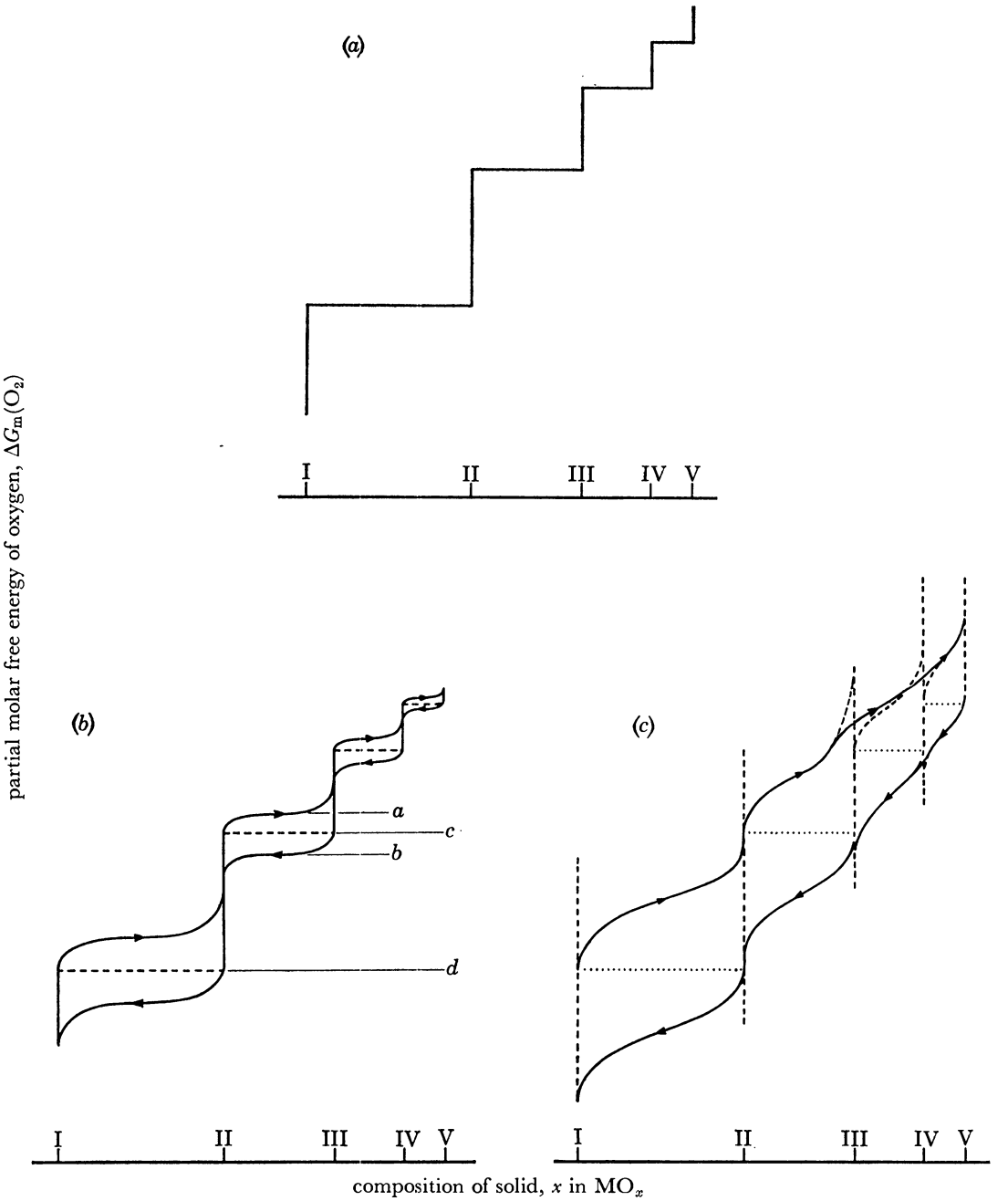

FIGURE 8. (*a*) Schematic equilibrium diagram of $\Delta G_m(O_2) = f(x)_T$ for a binary oxide system with five *independent* solid line phases. (*b*) Schematic diagram of $\Delta G_m(O_2) = f(x)_T$ for a binary oxide system with five *non-independent* solid line phases showing isolated hysteresis loops in the diphasic regions, cf. Pr+O and Tb+O. *ab* is the height of one loop, between phases II and III; *cd* is the stability range of phase II. The broken line represents the hypothetical situation that the phases are independent (cf. figure 8*a*). (*c*) Schematic diagram of $\Delta G_m(O_2) = f(x)_T$ for a binary oxide system in which *ab* is usually greater than *cd* (contrast figure 8*b*). The $\Delta G_m(O_2)$ ranges of the separate hysteresis loops (broken lines) overlap, and fuse together to give a composite loop (full line). The dotted line represents the hypothetical simple behaviour of independent solid phases.

Phenomenologically, the difference between the TiO_x system in this composition range and the lanthanoid oxides quoted above is simply that the degree of hysteresis (given by the height of a single loop: e.g. *ab* in figure 8*b*) is much greater in the former. The stability range of a phase (e.g. *cd* in figure 8*b*) is similar in the two cases. But, in PrO_x this is greater than the individual loop height ($cd/ab > 1$), whereas the converse is true for TiO_x ($ab/cd > 1$). Approximate values of the ranges *ab* and *cd* have been measured for PrO_x and this region of TiO_x, and they are listed in table 3.

Thus, in PrO_x there is always a range of $\Delta G_m(O_2)$ values between adjacent hysteresis loops, corresponding to a virtually pure, monophasic solid. In TiO_x this is not so, except at $x = 1.75$.

TABLE 3. A COMPARISON OF PHASE STABILITY RANGES AND HEIGHTS OF HYSTERESIS LOOPS IN THE SYSTEMS $PrO_x + O_2$ AND $TiO_x + O_2$

oxide	height of loop, *ab*†/kJ mol^{-1}	stability range of a single phase, *cd*†/kJ mol^{-1}
PrO_x	0.3	2 to 6
TiO_x	10	2.5 (at $n = 10$) to 25 (at $n = 4$)

† See figure 8*b*.

In these terms ($ab/cd > 1$) one may deduce the behaviour shown schematically in figure 8*c*. Clearly, *almost*-stationary compositions may appear *between* the compositions of stable line phases. (Before the phase reaction II → III is complete another reaction III → IV starts.) Superficially, they would resemble non-stoichiometric phases.

Thus, in the experiments, values of $n > 4$ are 'smeared out' to an extent which depends on the nature and history of the sample. The almost-stationary composition ranges are perhaps slightly narrower for single crystal than for powder samples. They are certainly narrower when this hysteresis loop is entered from lower compositions (runs 8 and 9) rather than from higher compositions (runs 4 and 6). This is presumably because the supposed 'reconstructive' transformation $Ti_3O_5 \rightarrow Ti_4O_7$ allows a relatively uncomplicated texture to obtain in Ti_4O_7 produced by oxidation. (Conversely, the change from (132) to (121) c.s. planes during reduction may perhaps confound an already confused domain texture in the crystals.) The observations on runs 8 and 9 (which are presumed to be the more significant) are as follows.

(i) In run 8 (figure 6*b*) steady masses occurred at $x = (1.8331 \pm 0.0002)$ in reduction, and $x = (1.8318 \pm 0.0002)$ in oxidation. Almost steady masses were also observed at the stationary compositions $x = 1.7965$ and 1.7968 (2 points) and $x = 1.7996$ to 1.8002 (3 points).

(ii) In run 9 (figure 7) somewhat 'less stationary' compositions appeared at $x = (1.799 \pm 0.004)$ and $x = (1.832 \pm 0.002)$ in oxidation, and $x = (1.876 \pm 0.004)$ and $x = (1.830 \pm 0.005)$ in reduction.

These observations may reasonably be interpreted as indicating slightly (phase-) impure Ti_5O_9 ($x = 1.8000$), Ti_6O_{11} ($x = 1.8333$) and Ti_8O_{15} ($x = 1.8750$). There was no indication of Ti_7O_{13} ($x = 1.8571$), and the suggestion of Ti_9O_{17} ($x = 1.8889$) in run 9 is not conclusive because the composition ($1.8876 \leqslant x \leqslant 1.8889$) was rather close to the reversal at $x = 1.8912$.

Temperature fluctuations in the cryostat were thought to vitiate data from run 8 and so, as already explained, they were virtually eliminated in a repeat run 9. It is interesting that the inflexions at the Andersson phase compositions are *less* steep in the latter. Perhaps the small temperature oscillations 'purify' a phase.

Because of its wide ($G_m(O_2)$) stability range (cf. table 3) Ti_4O_7 is particularly prominent as a line phase. In run 8 (figure 6*a*, *b*) it appears at $x = (1.7499 \pm 0.0004)$ in reduction and

$$x = (1.7499 \pm 0.0002)$$

in oxidation.† It is the only unequivocal line phase in this loop. The other (121) c.s. phase compositions (except $n = 7$) are manifest only as inflexions in the loop boundaries, more obvious in oxidation than in reduction. This is in stark contrast with the step function (like figure 8*a*) drawn by Morozova & Konopel'ko (1965) and also by Anderson & Khan (1970). The latter authors stated that they could detect no homogeneity range for any intermediate phase but, to their precision ($\delta x \approx \pm 0.0025$), the same is true for most of our data also, although it is not true at our higher level of precision. The composition widths of the inflexions corresponding to the Ti_nO_{2n-1} phases in figures 3, 5, 6*b* and 7 vary from ± 0.0004 to ± 0.0065. The mean is ± 0.0034; not much outside Anderson & Khan's precision.

If our interpretation of the data from runs 8 and 9 is correct, then the results of run 4 (figure 3; the (121) loop entered by reduction) are not very meaningful in this range. Steady masses and stationary compositions were observed only at $x = 1.8730$, 1.8700 in reduction, and $x = 1.8213$ in oxidation. It may be significant that the first is close to Ti_8O_{15} ($x = 1.8750$); and the third recalls the $n \approx 11/2$ values $x = 1.81_8$ (Bogdanova *et al.*) and $x = 1.82_0$ (Morozova & Konopel'ko), which Anderson & Khan also observed. However, the second seems meaningless, except in terms of the discussion above concerning figure 8*c*, and so perhaps the third is also. Its appearance *may* be connected with the 'reversal' at $x = 1.799$. (The almost stationary composition at the reversal is not significant, being merely a scanning curve inside the composite hysteresis loop, cf. § 4*a* (vi) and § 7*a*.)

The loop appears to close at $x \approx 1.90$, but its height is much reduced above $x \approx 1.875$. These compositions correspond to $Ti_{10}O_{19}$ and Ti_8O_{15}, and this is relevant to the discussion in § 7*b*. Here we will only remark that the (121) phase $Ti_{10}O_{19}$ was not detected by Andersson (1970), but has been observed in small amounts in electron diffraction studies (Bursill & Hyde 1971*b*). Thus the composition range of this hysteresis loop does correspond quite well to that of the known (121) c.s. structures.

(*c*) *The region* $1.93 \lesssim x \lesssim 1.98$

This composition range is inhabited by a second hysteresis loop and coincides reasonably well with that reported for the (132) c.s. family. Earlier electron diffraction studies (Bursill *et al.* 1969) indicated Ti_nO_{2n-1} with $15 \lesssim n \lesssim 36$, i.e. $1.933 \lesssim x \lesssim 1.972$. But more systematic investigations suggested (Bursill & Hyde 1971*b*) that only even values of n occurred; and that the minimum value was temperature dependent, being $n = 16$ ($x \simeq 1.938$) in samples quenched from 1300 K. This agrees fairly well with the observed loop closure at $x \approx 1.93$ at 1304 K. High n values cannot be accurately determined: electron microscopy (Bursill & Hyde 1971*a*) gave a maximum $n = 36$ or 37 ($x = 1.972$ or 1.973) in good agreement with the earlier $n \approx 35$ by diffraction. Magnification errors limit the accuracy in measuring the c.s. plane spacing to about $\pm 10\%$. The accuracy of the deduced n value is the same; and the maximum x is therefore 1.970 to 1.975. This is in satisfactory agreement with the observed loop closure at $x \approx 1.971$ in run 3 and $x \approx 1.980$ in run 4 (figures 4*b*, 3 and 9); especially when one recalls (§ 4) that, at high x values, the

† The reduction line at $x \approx 1.748$ in figure 6*a* is part of a 'scanning curve'. It occurred after apparently incomplete oxidation of $TiO_{\sim 1.73}$ to $TiO_{1.749}$ (cf. the discussion at the end of (*a*) above), and is probably $TiO_{1.7500}$ plus approx. 2.5% $TiO_{1.66}$.

PHILOSOPHICAL TRANSACTIONS OF THE ROYAL SOCIETY A MATHEMATICAL, PHYSICAL & ENGINEERING SCIENCES

path is very dependent on the details of the initial preparation. (Note how runs 1 and 2, in figure 4*a*, disagree at first but tend to coincide at lower x values (longer times): and how run 3, in figure 4*b*, disagrees with both. The starting compositions were $x = 1.9821$, 1.9834 and 1.9708 respectively.)

Figure 8*c* and the related discussion (§ 5*b*) suggest the strong possibility of considerable confusion in the texture of a crystal along this loop. Individual loops would correspond to $\Delta n = 2$, i.e. Δx varies from 0.0089 at $n = 14$ to 16 to 0.0016 at $n \approx 36$. Because the phase compositions are so similar† the stability range of each phase will be correspondingly small

$$(\Delta[\Delta G_{\mathrm{m}}(\mathrm{O}_2)] \approx 1\,\mathrm{kJ\,mol^{-1}}),$$

although the height of the loop is still very large ($\sim 10\,\mathrm{kJ\,mol^{-1}}$). Very clear inflexions are almost entirely restricted to the reduction legs (figures 3 and 4*a*). Some stationary compositions recur in all the runs; some do not. In addition to the expected even n values, many correspond very precisely to odd values of n in $\mathrm{Ti}_n\mathrm{O}_{2n-1}$. Some correspond quite accurately to $(n+\frac{1}{2})$ or $(n \pm \frac{1}{3})$, i.e. to integral values of n in $\mathrm{Ti}_n\mathrm{O}_{2n-2}$ or $\mathrm{Ti}_n\mathrm{O}_{2n-3}$. These correspondences and the very steep profiles on the 'steps' seem to us more than mere coincidence, but our compositional accuracy is still not high enough for a convincing analysis to be made. They may indicate ordered intergrowths of adjacent (132) phases.

It should also be pointed out that the step heights are usually between 0.65 and $1.5\,\mathrm{kJ\,mol^{-1}}$. They would therefore have remained undetected if the $\Delta G_{\mathrm{m}}(\mathrm{O}_2)$ increments had been $\lesssim 1\,\mathrm{kJ\,mol^{-1}}$, as in the work of Bogdanova *et al.*, Morozova & Konopel'ko, and Anderson & Khan. They appeared only when the increments were reduced to 0.25 to $0.5\,\mathrm{kJ\,mol^{-1}}$.

Thus at this stage, while the observations here are not surprising (not inconsistent with our other knowledge), neither are they fully understood. In particular the smooth profile of most of the oxidation leg in figure 3 seems rather strange. Presumably it is a scanning curve inside a more complete composite (132) hysteresis loop.

(*d*) *The region* $x \gtrsim 1.98$; *and the data of Zador* (1967) *and others*

In this composition range the oxygen potential varies rapidly with composition (figures 3, 4). The data are shown on a much enlarged composition scale in figure 9, which also includes results from some other workers (mainly for $x \gtrsim 1.99$). The data of Førland (1964), Moser *et al.* (1965) and Zador (1967) at high compositions, and interpolated to 1304 K, are in fair agreement (corresponding to a rather large experimental error). But, at first sight, they appear to differ greatly from our data: $\delta x = 0.0124$ at $\Delta G_{\mathrm{m}}(\mathrm{O}_2) = -400\,\mathrm{kJ\,mol^{-1}}$ (the respective values of δ in $\mathrm{TiO}_{2-\delta}$ being 0.0164 and 0.0040!) or, extrapolating, $\delta[\Delta G_{\mathrm{m}}(\mathrm{O}_2)] \approx 80\,\mathrm{kJ\,mol^{-1}}$ at $x = 1.989$. We believe that the apparent disagreement is readily resolved in the following way.

In very slightly reduced rutile ($x \gg 1.99$) the oxygen deficiency is accommodated by disordered {132} c.s. planes. Apparently, these slowly aline into parallel ordered groups (lamellae) in which the composition approaches $x \approx 1.98$ as they grow (Bursill & Hyde 1971*a*). Thus, in the range $1.98 \lesssim x \lesssim 2.00$ the equilibrium texture consists of lamellae of c.s. planes in a rutile matrix which has x close to 2.00. The lamellar composition is a function of its size (and therefore of the crystal's mean composition $\bar{x}$) but, if we ignore this as a second-order effect, the crystal may be described as having a micro-domain texture with lamellae of the highest order (132) c.s. phase dispersed in the rutile matrix. In classical terms the solid is diphasic, and the equilibrium system would be

† The Δx values correspond to changes of only 0.46 and 0.08 % in the O/Ti ratio.

univariant. Because of the hybrid texture, the variation of lamellar composition with size and $\bar{x}$, the variation in the concentration of c.s. planes, and the slowness of the ordering process we would expect a hysteresis loop in this region. Unfortunately sufficient thermodynamic data to test this hypothesis (by completely circumnavigating the loop) are not available; but there is quite a lot of circumstantial evidence consistent with the hypothesis. We consider Zador's (1967) paper first.

(i) Because of the initial treatment (§ 3 (*b*)) all our starting samples ($x \approx 1.98$) were prepared in oxidation. On the other hand, all Zador's data are in reduction. Both sets are included in figure 9, and it is clear that no strain is required to make them fall on to one hysteresis loop. In both cases the reduction points appear to tend asymptotically to a lower boundary of the loop that is approximately horizontal at $\Delta G_m(O_2) \approx -440\,\mathrm{kJ\,mol^{-1}}$.

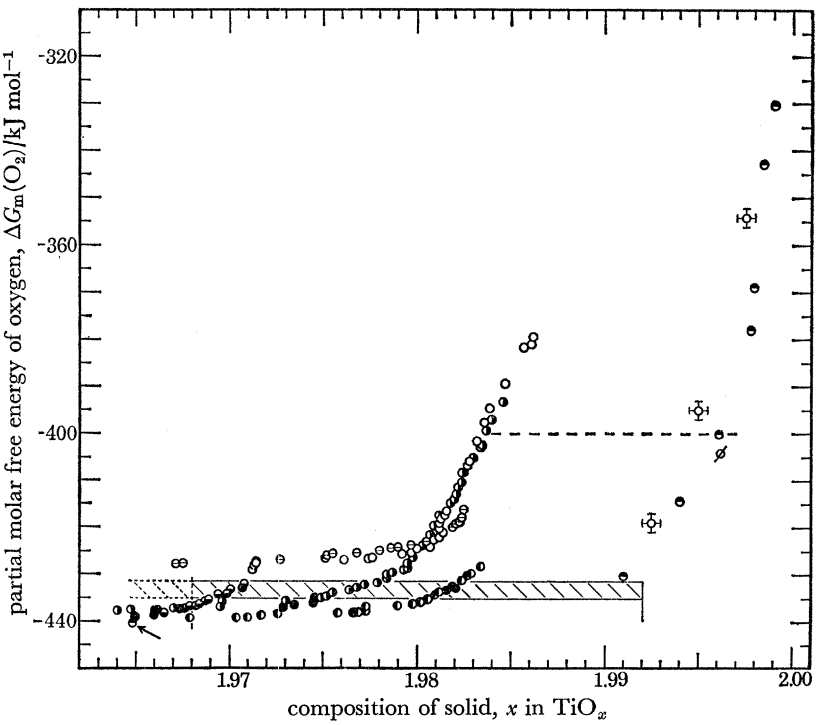

FIGURE 9. The isothermal (1304 K) relation between $\Delta G_m(O_2)$ and x = O/Ti in the composition range $1.964 \lesssim x \lesssim 1.999$.

Data from the present work are: (●) run 1, reduction; (◐) run 2, reduction; run 3, (◒) reduction, (○) oxidation; run 4, (◑) reduction, (⊖) oxidation. In addition, (◓) are 1304 K values interpolated from Zador's (1967) data (note especially the additional point from Zador's (1969) thesis indicated by an arrow at $x \approx 1.96$); ∅ is a point interpolated from Førland's (1964) results. The hatched band is interpolated from Blumenthal & Whitmore (1963); the points ⊕ from Moser *et al.* (1965). The graph suggests the existence of a large hysteresis loop in the region $1.98 \lesssim x \lesssim 1.998$ between the highest ordered (132) c.s. phase and slightly disordered oxygen-deficient rutile. Note how *all* the reduction paths tend asymptotically to a line $\Delta G_m(O_2) \doteqdot -440\,\mathrm{kJ\,mol^{-1}}$. A hypothetical 'equilibrium' line for coexisting independent phases in this region is proposed at $\Delta G_m(O_2) = -400\,\mathrm{kJ\,mol^{-1}}$, and is shown as a broken horizontal line.

(ii) The $TiO_{1.991}$ isopleth in Zador's (1967) Figure 1 appears to be the boundary of a 'diphasic region' ($\Delta G_m(O_2)$ independent of x) at 1304 K. This is the lowest of her (1967) points in figure 9, at $\Delta G_m(O_2) = -430\,\mathrm{kJ\,mol^{-1}}$ which is only $10\,\mathrm{kJ\,mol^{-1}}$ from the 'horizontal' in (i).

(iii) From her values of the partial molar enthalpy of oxygen Zador deduced that, for $x < 1.991$, 'the dilute solution model no longer holds': i.e. the behaviour is markedly different from that at higher compositions. This change of behaviour is consistent with (i) and (ii).

(iv) She observed that 'about and below $\Delta G_m(O_2) = -418\,kJ\,mol^{-1}$ the e.m.f. [of her electrochemical cell] was showing a very slow drift of about 2 or 3 mV per day towards more positive values, which suggests a very small but continuous pick-up of oxygen from the surrounding atmosphere'. We suggest as an alternative explanation consistent with the hypothesis advanced above and all the available information including Zador's two-phase $x = 1.991$ line and the electron microscopy evidence, that the slow drift towards higher $\Delta G_m(O_2)$ values probably occurs at constant composition and is due to a slow passage towards equilibrium, especially the slow aggregation and ordering of the initially highly disordered {132} c.s. planes; i.e. the lower phase boundary of $TiO_{2-\delta}$ is at $\Delta G_m(O_2) \geqslant -418\,kJ\,mol^{-1}$. (Cf. our estimate of about $-400\,kJ\,mol^{-1}$.) We observed a similar drift in oxidation in run 3 for $\Delta G_m(O_2) \gtrsim -400\,kJ\,mol^{-1}$; whereas no drift was detected in the range $-424 \lesssim \Delta G_m(O_2) \lesssim -400\,kJ\,mol^{-1}$. Furthermore:

(v) There is satisfactory agreement between the observations of Blumenthal & Whitmore (1963), Moser *et al.* (1965) and the above interpretation of behaviour in this region. Moser *et al.* deduced that the solid was monophasic for $x > 1.992$: their data (interpolated at 1304 K) agree with Zador's to within 0.001 in x, their accuracy being $\delta x = \pm 0.0005$. Blumenthal & Whitmore deduced a diphasic solid region (i.e. they observed univariant behaviour) from $x = 1.992$ to $1.957 < x \leqslant 1.968$: the reproducibility of their cell e.m.f. was rather poor ($\pm 5\,mV = 1.9\,kJ\,mol^{-1}$ in $\Delta G_m(O_2)$), as would be expected if they were experiencing the 'drift' reported by Zador. Interpolating at 1304 K, their 'diphasic equilibrium' (which we interpret as being at or near the bottom of the hysteresis loop) was at $\Delta G_m(O_2) = (-433.2 \pm 1.9)\,kJ\,mol^{-1}$. This compares reasonably well with the approx. $-440\,kJ\,mol^{-1}$ in (i), $-430\,kJ\,mol^{-1}$ in (ii), and the other data in figure 9.

Further data, important in the present context, are available from Zador's (1969) thesis: an isopleth at a lower composition, $x = 1.9648$. Interpolated to 1304 K, her value of

$$\Delta G_m(O_2) = (-440.4 \pm 0.8)\,kJ\,mol^{-1}$$

may be compared with our

$$\Delta G_m(O_2) = (-439.5 \pm 2.0)\,kJ\,mol^{-1}$$

at $x = 1.9649$ (run 1) and

$$\Delta G_m(O_2) = (-437.6 \pm 2.0)\,kJ\,mol^{-1}$$

at $x = 1.9647$ (run 4): see figure 9. Thus, at the one point where our data and Zador's overlap, so that a direct comparison can be made, the agreement is excellent: $\pm 1\,kJ\,mol^{-1}$, which is well within experimental error.

(e) *Comparison of* $\Delta G_m(O_2)$ *values with those of other workers,* $x < 1.98$

Our work overlaps most with that of Bogdanova *et al.* (1963) and Morozova & Konopel'ko (1965). Within their uncertainties, which we assess as approx. $5\,kJ\,mol^{-1}$ in $\Delta G_m(O_2)$ and 0.007 in x, their data are in mutual agreement. On the other hand, at the same compositions, our $\Delta G_m(O_2)$ values are consistently lower than theirs by about $7\,kJ\,mol^{-1}$ in oxidation and $17\,kJ\,mol^{-1}$ in reduction. We therefore checked our technique by measuring $x = f\{\Delta G_m(O_2)\}_T$ for CeO_x in $(H_2 + H_2O)$ gas buffers at 1296 K: comparing the results with those of Bevan & Kordis (1964) on the same system at the same temperature. A ceria sample of nominal purity 99.9% gave $\Delta G_m(O_2)$ values $21\,kJ\,mol^{-1}$ higher than those of Bevan & Kordis, but purification by the method of Klinaev & Senyavin (1955) reduced the discrepancies to $\gtrsim 5.0\,kJ\,mol^{-1}$; i.e. gave agreement to within experimental error.

Conceivably the discrepancies for TiO_x could also be due to different purities, but our single

crystal rutile was less pure than our powder samples (cf. table 1) whereas, in similar experiments, $\Delta G_m(O_2)$ values agreed to $\gtrsim 0.84\,kJ\,mol^{-1}$. We believe that thermal segregation in the gas buffer is a more likely source of the discrepancy between the sets of TiO_x data. Too low a gas flow rate would give an apparent value of $\Delta G_m(O_2)$ higher than the true value. We confirmed that our flow rate was sufficiently high (§ 3*b*): the possibility is not commented on in the papers of the other workers.

Comparison with the data of Anderson & Khan (1970) is rather difficult; their data points are really too sparse for an accurate determination of $\Delta G_m(O_2)$ values for pairs of coexisting solid phases. The values they have deduced, interpolated to 1304 K, are comparable with those of the Russian workers, and higher than ours. This is confirmed by their value of $\Delta G^{\ominus}$ for

$$Ti_4O_7 + O_2 = Ti_5O_9,$$

which yields a $\Delta G_m(O_2)$ value about $3\,kJ\,mol^{-1}$ higher than our oxidation value and about 13 or $14\,kJ\,mol^{-1}$ higher than our reduction value in the same composition range. The gas flow rate they quote seems rather low; so that thermal segregation is a possibility. Nevertheless, our data are consistently lower than those from all three of these research groups, and also lower than the data from electrochemical cells by Golubenko & Rezukhina (1967) and Vasil'eva & Shaulova (1969) which cannot be subject to thermal segregation errors. A short extrapolation of the equations of Golubenko & Rezukhina to 1304 K yields $\Delta G_m(O_2)$ values about 10 to $20\,kJ\,mol^{-1}$ higher than ours (cf. figure 3), while those of Vasil'eva & Shaulova are about 10 to $40\,kJ\,mol^{-1}$ higher than ours. In table 4, $\Delta G_m(O_2)$ values calculated from the data of Vasil'eva & Shaulova and Anderson & Khan are listed together with our 'mean values', calculated in the manner described in § 6*a* below. The agreement is not very good. It is also possible that the discrepancies are due to errors in measuring the sample temperature.

TABLE 4. A COMPARISON OF $\Delta G_m(O_2)$ VALUES FOR SEVERAL DIPHASIC MIXTURES FROM THE PRESENT WORK WITH THOSE OF VASIL'EVA & SHAULOVA (1969) AND ANDERSON & KHAN (1970)

	$-\Delta G_m(O_2)/kJ\,mol^{-1}$ at 1304 K		
phase mixture	present work	Vasil'eva & Shaulova	Anderson & Khan
$Ti_3O_5 + Ti_4O_7$	509.3 ± 2.0	468.7 ± 1.5	—
$Ti_4O_7 + Ti_5O_9$	482.2	—	474.7
$Ti_5O_9 + Ti_6O_{11}$	477.5	—	561.8†
$Ti_6O_{11} + Ti_7O_{13}$	466.2	456.58 ± 0.09	—
$Ti_8O_{15} + Ti_9O_{17}$	459.4	447.79 ± 0.04	—

† This value is clearly wrong, probably because of a misprint or arithmetical error in their paper (see text, § 6*b*).

On the other hand, there *are* data in reasonable agreement with our own.

(i) We have already referred (in § (*d*)) to the excellent agreement between our results and Zador's reduction point at $x = (1.9648 \pm 0.0001)$ and $T = 1304$ K. This may also imply agreement with the data of Førland (1964) and Moser *et al.* (1965) at higher compositions (if our explanation of behaviour in the region $x \gtrsim 1.98$ is accepted). Certainly we are in quite good agreement with the results of Blumenthal & Whitmore (1963) in their 'diphasic region'. Their $\Delta G_m(O_2)$ value (interpolated to 1304 K) falls nicely between our oxidation and reduction asymptotes, which are themselves separated by about $11\,kJ\,mol^{-1}$ (figure 9).

(ii) We have also mentioned the agreement between some data we acquired from

$$CeO_x\,(s) + H_2\,(g) + H_2O\,(g)$$

and those of Bevan & Kordis (1964).

(iii) Less directly, from our data we have deduced (§ 6) a value for the standard free energy of the reaction $2Ti_3O_5 + O_2 = 6TiO_2$ (rutile) at 1304 K. Comparing this with the corresponding quantity computed from the JANAF tables (Stull 1965) reveals that, on the average, our $\Delta G_m(O_2)$ values are *too high* by (6.6 ± 3.6) kJ mol^{-1}, rather than too low.

Hence, we have no sound reason for doubting the accuracy of our results.

Porter (1965) also attempted to explore the thermodynamics of the higher titanium oxides. His technique was to equilibrate solid TiO_x with a gas buffer at high temperature (1600 to 1700 K): the phase(s) present were identified by X-ray powder diffraction on the rapidly quenched sample. Its reliability depends on effective quenching, and our experience indicates that this is impossible: that the solid would oxidize while cooling. This is consistent with his $\Delta G_m(O_2)$ values (extrapolated to 1304 K) being much lower than ours: by about (40 ± 10) kJ mol^{-1} over the whole composition range from Ti_3O_5 to rutile.

6. Derived thermodynamic properties

(*a*) *Standard free energies of formation of* Ti_3O_5 *and the ordered intermediate phases*

By combining our data with those of Zador (which are probably the most reliable at higher compositions) we can calculate the standard free energy change $\Delta G^{\ominus}$ (1304 K) for

$$TiO_x + (1 - \tfrac{1}{2}x)\,O_2 = TiO_2\ (\text{rutile}) \qquad (1)$$

for $\frac{5}{3} \leqslant x < 2$.† Inaccuracy is introduced by the hysteresis that obtained in our experiments, but we attempted to minimize this by the following procedure.

The data from run 9 ($1.7500 \leqslant x \leqslant 1.8900$) and run 4 ($1.8900 \leqslant x \leqslant 1.9830$) were combined with those from Zador (1967) ($1.991 \leqslant x \leqslant 1.9991$, interpolated to 1304 K and extrapolated to $x = 2.0000$) and plotted on a large scale as $\Delta G_m(O_2)$ against x. The (121) and (132) hysteresis loops were divided by a vertical line (x = constant) at the *ideal* composition of each of the crystallographically plausible ordered intermediate phases Ti_nO_{2n-1} from $n = 4$ to 30, and then at intervals $\Delta n = 5$ up to $n = 50$ (which corresponds to an upper composition limit for these phases of $x = 1.9800$). The (constant) equilibrium value of $\Delta G_m(O_2)$ for the coexistence of two adjacent phases must lie within the hysteresis loop between them: we assumed it also lies within the composite loops. Its value was taken as that of the $\Delta G_m(O_2)$ = constant line which divided the loop section (between adjacent constant composition lines) into equal areas. The proposed third loop, $1.9836 \leqslant x \leqslant 1.9960$ was divided by $\Delta G_m(O_2) = -400$ kJ mol^{-1}: which we estimate to be the best 'equilibrium value'.‡ In the remaining regions, other than Ti_3O_5 to Ti_4O_7,

$$\Delta G_m(O_2) = f(x)_T$$

is almost reversible. Mean values were therefore taken at closely spaced compositions.

† We elected to use TiO_2 (rutile) as the reference compound rather than Ti_3O_5 because there seems to us to be some doubt about characterizing the latter; cf. § 5*a*.

‡ This is the most uncertain $\Delta G_m(O_2)$ value, but the composition range is so small that no reasonable change could significantly affect the derived $\Delta G^{\ominus}$ values. A shift of 100 kJ mol^{-1} in the former changes the latter by no more than 0.65 kJ (mol TiO_x)$^{-1}$.

PHILOSOPHICAL TRANSACTIONS OF THE ROYAL SOCIETY A MATHEMATICAL, PHYSICAL & ENGINEERING SCIENCES

Hence (assuming that the standard free energy of formation of the solid is independent of pressure) we are able to estimate the increments $\Delta G^{\ominus}$ across any composition interval Δx:

$$\Delta G^{\ominus} = \Delta G_{\mathrm{m}}(\mathrm{O}_2)\,\Delta x$$

and/or

$$\Delta G^{\ominus} = \int_{x}^{x+\Delta x} \Delta G_{\mathrm{m}}(\mathrm{O}_2)\,\mathrm{d}x.$$

In this way $\Delta G^{\ominus}$ was calculated for reaction (1) for $1.7500 \leqslant x < 2.0000$.

In a similar way $\Delta G^{\ominus}$ for $\frac{1}{3}\mathrm{Ti_3O_5} + \frac{1}{24}\mathrm{O_2} = \frac{1}{4}\mathrm{Ti_4O_7}$ was deduced from the 'dead zone' values of $\Delta G_{\mathrm{m}}(\mathrm{O_2})$ at $x = 1.705$, i.e. near the centre of the diphasic region (see § 5*a*). The weighted mean was

$$\Delta G_{\mathrm{m}}(\mathrm{O_2}) = -(509.3 \pm 2.0)\ \mathrm{kJ\ mol^{-1}}.$$

Taking into account the uncertainties listed in table 2 this yields, for the ideal compositions

$$\mathrm{TiO_{1.6666}} + 0.04166\dot{6}\ \mathrm{O_2} = \mathrm{TiO_{1.7500}},$$

$$\Delta G^{\ominus}\ (1304\,\mathrm{K}) = -(21.22 \pm 0.17)\ \mathrm{kJ\ mol^{-1}}.$$

This extends the range of values of $\Delta G^{\ominus}$ for reaction (1) to $\frac{5}{3} \leqslant x < 2$.

We have also calculated the standard integral free energies of mixing one (total) mole of atoms of titanium plus oxygen, G^{*}_{M}, from these data;† together with the corresponding mole fractions of oxygen, $x_0^{*} = x/(1+x)$. $G^{*}_{M} = G^{\ominus}_{\mathrm{m}}(\mathrm{TiO}_x)/(1+x)$, where $G^{\ominus}_{\mathrm{m}}(\mathrm{TiO}_x)$ is the standard molar free energy of formation of TiO_x, i.e. $\Delta G^{\ominus}$ for $\mathrm{Ti\,(s)} + \frac{1}{2}x\,\mathrm{O_2\,(g)} = \mathrm{TiO}_x\,\mathrm{(s)}$. $G^{\ominus}_{\mathrm{m}}(\mathrm{TiO}_x)$ values rely on a reference $G^{\ominus}_{\mathrm{m}}(\mathrm{TiO_2},\ \mathrm{rutile}) = -708.025\,\mathrm{kJ\ mol^{-1}}$, which we computed from data in the JANAF tables. Obviously the G^{*}_{M} values also rely on this reference. We also calculated values of an analogous function which does *not* depend on other data, namely $G^{\dagger}_{\mathrm{M}}$, the standard integral free energy of mixing one mole of atoms starting with $\mathrm{Ti_3O_5\,(s)}$ and $\mathrm{O_2\,(g)}$ at 1 atm pressure; together with the corresponding 'mole fraction of oxygen atoms' (from $\mathrm{O_2}$ molecules)

$$x_0^{\dagger} = (x - 1.6666\dot{})/(x+1).$$

The reference point here is $G^{\dagger}_{\mathrm{M}}(\mathrm{Ti_3O_5}) = 0$. In general,

$$G^{\dagger}_{\mathrm{M}} = \{G^{\ominus}_{\mathrm{m}}(\mathrm{TiO}_x) - G^{\ominus}_{\mathrm{m}}(\mathrm{TiO_{1.66\dot{}}})\}/(x+1).$$

All these data are collected in table 5, which also includes the corresponding quantities for $\mathrm{Ti_2O_3}$, again calculated from data in the JANAF tables.

Graphs of $G^{*}_{\mathrm{M}} = f(x_0^{*})_T$ and $G^{\dagger}_{\mathrm{M}} = f(x_0^{\dagger})_T$ are valuable ways of summarizing and depicting the thermodynamic properties and equilibrium behaviour of multiphase binary systems (cf. Darken & Gurry 1953). They are plotted in figure 10. Note the very small free energy changes for a reaction in which any two next nearest phases produce the intermediate phase,

$$n + (n+2) = 2(n+1),$$

especially for $x \gtrsim 1.83$. This emphasizes the likelihood that preparations will result in phase mixtures rather than pure phases, as we observe in practice (Bursill *et al.* 1969; Bursill & Hyde 1971*b*). For $\mathrm{Ti_6O_{11}} + \mathrm{Ti_8O_{15}} = 2\mathrm{Ti_7O_{13}}$ the standard free energy change is

$$\Delta G^{\ominus} = \Delta G^{*}_{\mathrm{M}} = \Delta G^{\dagger}_{\mathrm{M}} = -5.2\,\mathrm{J}$$

per mole of atoms, i.e. $-10_4\,\mathrm{J}$ per mole of $\mathrm{Ti_7O_{13}}$ (all at 1304 K).

† They are Darken & Gurry's (1953) 'integral molar free energy of mixing of the components, F^{*}'.

TABLE 5. THERMODYNAMIC FUNCTIONS OF THE HIGHER TITANIUM OXIDES AT 1304 K

n in Ti_nO_{2n-1}	x in TiO_x	$-\Delta G_m(O_2)$ kJ mol^{-1}	$-\Delta G^{\ominus}$ kJ mol^{-1}	$-G_m^{\ominus}(TiO_x)$ kJ mol^{-1}	$x_0^* = \frac{x}{1+x}$	$-G_M^*$ kJ mol^{-1}	$x_0^\dagger = \frac{x-1.6}{1+x}$	$-G_M^\dagger$ kJ mol^{-1}
2	1.50000			**552.064**	0.60000	**220.826**	—	—
		(**918.4**)	**76.536**	**628.600**		**235.725**		
3	1.66667			629.730	0.62500	236.149	0	0
		509.3	21.221					
4	1.75000			650.950	0.63636	236.709	0.03030	7.717
		482.2	12.055					
5	1.80000			663.005	0.64286	236.788	0.04762	11.884
		477.5	7.958					
6	1.83333			670.964	0.64706	236.811	0.05882	14.553
		466.2	5.550					
7	1.85714			676.514	0.65000	236.780	0.06667	16.374
		463.3	4.137					
8	1.87500			680.650	0.65217	236.748	0.07246	17.712
		459.4	3.190					
9	1.88889			683.840	0.65385	236.714	0.07692	18.731
		456.0	2.534					
10, *s*	1.90000	455.0		686.374	0.65517	236.681	0.08046	19.533
			1.817					
—, *s*	1.90800	453.8		688.191	0.65612	236.655	0.08299	20.104
			1.813					
—, *s*	1.91600	452.7		690.005	0.65706	236.627	0.08551	20.670
			1.807					
—, *s*	1.92400	450.6		691.911	0.65800	236.598	0.08801	21.232
			1.028					
14, *s*	1.92857	449.1		692.840	0.65854	236.579	0.08943	21.550
		445.3	1.988					
16	1.93750			694.828	0.65957	236.537	0.09220	22.161
		441.2	1.532					
18	1.94444			696.359	0.66038	236.499	0.09434	22.629
		437.9	1.217					
20	1.95000			697.576	0.66102	236.466	0.09605	22.999
		436.3	0.992					
22	1.95455			698.567	0.66154	236.438	0.09744	23.299
		435.1	0.824					
24	1.95833			699.391	0.66197	236.414	0.09859	23.548
		433.7	0.695					
26	1.96154			700.086	0.66234	236.393	0.09957	23.757
		433.5	0.596					
28	1.96429			700.682	0.66265	236.375	0.10040	23.936
		432.6	0.515					
30	1.96667			701.197	0.66292	236.359	0.10112	24.090
		432.3	1.030					
35	1.97143			702.226	0.66346	236.326	0.10256	24.398
		431.2	0.770					
40	1.97500			702.996	0.66387	236.301	0.10364	24.627
		429.3	0.596					
45	1.97778			703.592	0.66418	236.281	0.10448	24.805
		427.5	0.475					
50, *s*	1.98000	424.4		704.068	0.66443	236.264	0.10515	24.946
			0.421					
—, *s*	1.98200	417.0		704.489	0.66466	236.247	0.10575	25.070
			0.328					
—, *s*	1.98360	400.0		704.816	0.66483	236.230	0.10623	25.167
		400.0	2.480					
—, *s*	*1.99600*	400.0		*707.296*	0.66622	236.080	0.10992	25.890
			0.198					
—, *s*	*1.99700*	*390.0*		*707.494*	0.66633	236.067	0.11022	25.947
			0.190					
—, *s*	*1.99800*	*370.0*		*707.684*	0.66644	236.052	0.11052	26.002
			0.176					
—, *s*	*1.99900*	*330.0*		*707.860*	0.66656	236.032	0.11082	26.052
			~0.165					
—, *s*	2.00000	~252.2		**708.025**	0.66667	**236.008**	0.11111	26.098

For footnotes see opposite page.

PHILOSOPHICAL TRANSACTIONS OF THE ROYAL SOCIETY A MATHEMATICAL, PHYSICAL & ENGINEERING SCIENCES

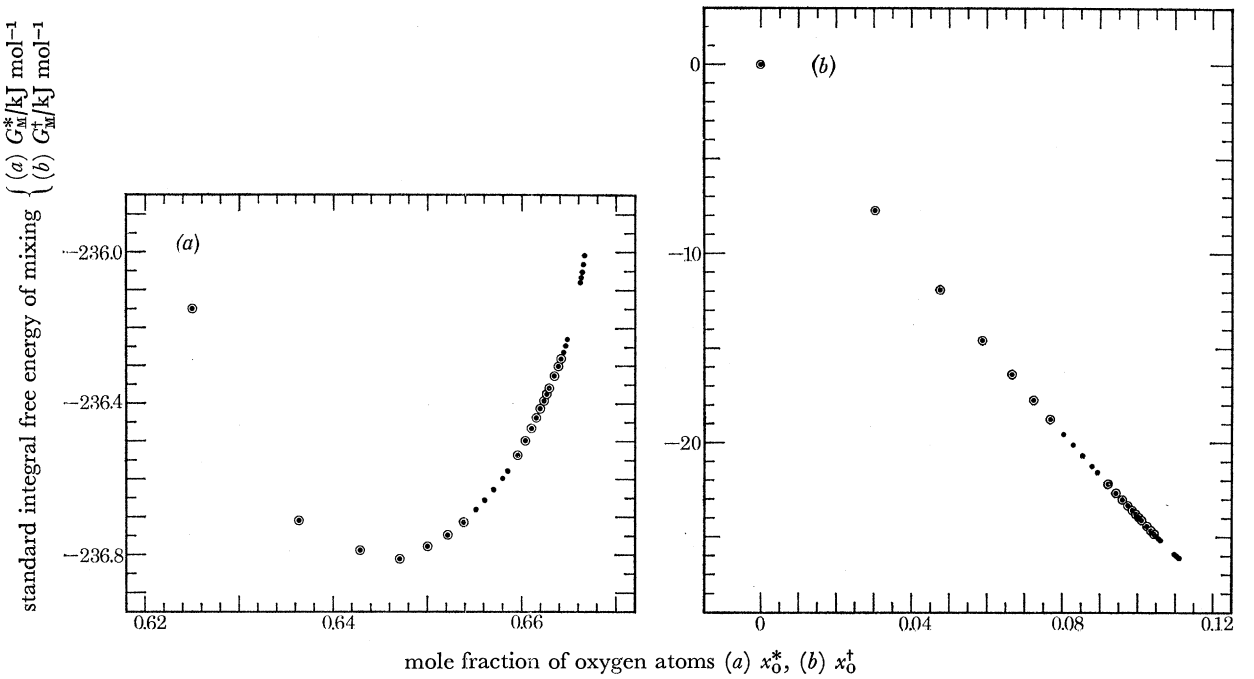

FIGURE 10. Standard integral free energy of mixing (per mole of total atoms) as a function of the mole fraction of added oxygen atoms at 1304 K: the data are listed in table 5. (*a*) G_M^* for mixing Ti(s) + O_2(g), $x_O^* = x/(1+x)$; (*b*) $G_M^\dagger$ for mixing Ti_3O_5(s) + O_2(g), $x_O^\dagger = (x-5/3)/(1+x)$. The results in (*a*) are based on the standard free energy of formation of TiO_2 (rutile) from the JANAF tables. ⊙, line phases; ●, 'solid solution'.

(*b*) *Comparison of standard free energies with those from other sources*

The JANAF tables (Stull 1956) contain values for the standard free energy of formation of Ti_3O_5 and TiO_2 (rutile). Taken together they give

$$\tfrac{1}{3}Ti_3O_5 + \tfrac{1}{6}O_2 = TiO_2\ \text{(rutile)}, \quad \Delta G^\ominus(1304\,\text{K}) = -79.4\,\text{kJ mol}^{-1};$$

compared with $\Delta G^\ominus(1304\,\text{K}) = -(78.3 \pm 0.6)\,\text{kJ mol}^{-1}$ calculated from our data, in the way described in the last section. This measure of agreement justifies the, admittedly rather bold, assumptions in our calculations. It attests to the usefulness of the data in table 5 and, as already mentioned (at the end of § 5*e*), lends some support to the accuracy of our $\Delta G_m(O_2)$ values.

Column 1: *s* indicates a composition in an assumed homogeneous range of 'solid solution'.

Column 3: $\Delta G_m(O_2)$ is the relative partial molar free energy $(G_m - G_m^\ominus)$ of O_2(g) in (hypothetical) equilibrium with the solid phase or phases.

Column 4: $\Delta G^\ominus$ is the standard free energy change per mole of TiO_x for the appropriate composition increment from the previous to the following phase, i.e. for

$$TiO_{x_1} + \tfrac{1}{2}(x_2 - x_1)\ O_2 = TiO_{x_2}.$$

Column 5: $G_m^\ominus(TiO_x)$ is the standard molar free energy of formation of TiO_x.

Column 7: G_M^* is the standard integral free energy of mixing Ti(s) and O_2(g) to give one mole of atoms as TiO_x, i.e. the standard free energy change per mole for

$$(1-x_0^*)\ Ti(s) + \tfrac{1}{2}x_0^*\ O_2(g) = (1-x_0^*)\ TiO_x(s),$$

where x_0^* is the mole fraction of oxygen atoms.

Column 9: $G_M^\dagger$ is the standard integral free energy of mixing Ti_3O_5(s) and O_2(g) to give one mole of atoms as TiO_x, i.e. the standard free energy change per mole for

$$\tfrac{1}{8}(1-x_0^\dagger)\ Ti_3O_5(s) + \tfrac{1}{2}x_0^\dagger\ O_2(g) = \tfrac{3}{8}(1-x_0^\dagger)\ TiO_x(s),$$

where $x_0^\dagger$ is the mole fraction of added oxygen atoms.

The figures in bold type are interpolated from the JANAF tables (Stull 1965).

The figures in italics are from Zador (1967).

PHILOSOPHICAL TRANSACTIONS OF THE ROYAL SOCIETY A MATHEMATICAL, PHYSICAL & ENGINEERING SCIENCES

Interpolated to 1304 K the equations of Anderson & Khan (1970) yield:

$$TiO_{1.750} + 0.025O_2 = TiO_{1.800}, \quad \Delta G^{\ominus} = -11.86_7\,\mathrm{kJ\,mol^{-1}};$$

$$TiO_{1.800} + 0.016O_2 = TiO_{1.833}, \quad \Delta G^{\ominus} = -9.36_4\,\mathrm{kJ\,mol^{-1}}.$$

These may be compared with our values of $-12.05_5\,\mathrm{kJ\,mol^{-1}}$ and $-7.95_8\,\mathrm{kJ\,mol^{-1}}$ for the same reactions. The first is in fair agreement.† The second value is clearly wrong; presumably because of an arithmetical or printing error since their isotherms show that $\Delta G_m(O_2)$ increases with increasing x, whereas the value of $\Delta G_m(O_2)$ derived from this $\Delta G^{\ominus}$ is anomalously low (cf. table 4). (The comparison is not affected by Anderson & Khan's deduction that $Ti_{11}O_{20} = TiO_{1.818}$ exists between the phases Ti_5O_9 and Ti_6O_{11} involved in this second reaction.)

7. A structural explanation for the thermodynamic behaviour in the composition range $1.75 \leqslant x \lesssim 1.98$

(With L. A. Bursill and D. K. Philp)

We reduce the problem to two questions.

(1) Why is the hysteresis so great in the (121) and (132) loops?

(2) Why is it so much less in the intermediate region $1.90 \lesssim x \lesssim 1.93$?

Anderson & Khan (1970) suggested that the rate-determining step in oxidation or reduction is probably the lateral migration of c.s. planes. If this were so it would also be the cause of the observed hysteresis. But, lateral migration is necessary not only to adjust the spacing of c.s. planes but also to rotate them between the (121) and (132) orientations in the intermediate region where there is almost no hysteresis. Hence the observed gross hysteresis in the loops cannot be explained in this way. We propose an alternative explanation which is consistent with both the thermodynamic and electron microscope observations, and also with plausible models for phase reaction mechanisms (Bursill & Hyde 1972*a*, *b*).

The first question could be rephrased as 'Why is the hysteresis in the loops so much greater for TiO_x than for PrO_x?' It is about $10\,\mathrm{kJ\,mol^{-1}}$ in $\Delta G_m(O_2)$ for the former, compared with $0.3\,\mathrm{kJ\,mol^{-1}}$ for the latter. In the intermediate region it is comparable (0.5 to $1.0\,\mathrm{kJ\,mol^{-1}}$ for TiO_x).

(*a*) *A structural explanation of the gross hysteresis*

Electron micrographs only very rarely reveal a c.s. plane that ends *within* a TiO_x crystal. They are almost invariably continuous: across twin boundaries, or even domain boundaries between different structures (Bursill *et al.* 1969; Terasaki & Watanabe 1971; Bursill & Hyde 1971*a*, 1972*b*). This implies a high energy for the dislocation bounding a c.s. plane.

It follows that an excess chemical potential would be needed to generate or annihilate a c.s. plane (and these are essential to reduction or oxidation in either loop). Hence reversing the reaction path (from oxidation to reduction or vice versa) should reveal a $\Delta G_m(O_2)$ interval in which no reaction occurs: i.e. a 'stationary composition' should result, rather than a normal scanning curve. In this interval the oxygen potential would be too low for c.s. planes to be eliminated, but too high for them to be created. This is exactly what is observed (point (iv) in §4*a*).

† Although, of course, the apparently small discrepancy in $\Delta G^{\ominus}$, $0.18_8\,\mathrm{kJ\,mol^{-1}}$, leads to a reasonably large discrepancy in $\Delta G_m(O_2)$, namely $7.5_2\,\mathrm{kJ\,mol^{-1}}$.

A similar energy barrier cannot occur in the lanthanoid oxide systems PrO_x and TbO_x, because their intermediate structures are derived from the fluorite-type parent by the 'ordering of anion vacancies', rather than by c.s. (Brauer 1966).

But the most persuasive arguments to support the hypothesis come from a consideration of the second question, to which we now turn.

(*b*) *Thermodynamics and structure in the region* $1.90 \lesssim x \lesssim 1.93$

If our hypothesis is correct, the absence of gross hysteresis implies that no c.s. planes are created or destroyed when this region is traversed. Composition changes must therefore be accommodated entirely by changing the c.s. plane type, from (121) to (132) or vice versa; and the number of c.s. planes in a crystal will be constant throughout. Hence the c.s. plane spacing D_{sp} will also be constant.† At the interface between (121) and (132) c.s. domains the c.s. planes will be 'bent' through 0.20 rad. Electron diffraction studies of samples annealed at 1300 K and then quenched showed that, as the composition falls in this region $n = 16$ (132) changes to $n = 9$ (121). The corresponding *room temperature* D_{sp} values are $1.619 \rightarrow 1.460$ nm; a deviation of approx. -10%.‡ (Annealing at 1673 K and quenching gave $n = 12$ (132) $\rightarrow n = 8$ (121), with D_{sp} values $1.205 \rightarrow 1.291$ nm; a deviation of about $+7\%$.) At first sight this would seem to suggest that, while not grossly in error, the consequences deduced from our hypothesis are not entirely correct. However, it is not obviously *essential* that the change be between *integral n* values (although it is only these that could be unambiguously identified from their diffraction patterns). Indeed, it is most unlikely that D_{sp} = constant could be *exactly* satisfied by *any* pair of integral n values. For the moment we can only conclude that $D_{sp} \approx$ constant across this region, and return our attention to the thermodynamic observations.

The relevant data are from run 4. Figure 3 reveals that after traversing this intermediate range in which there is relatively little hysteresis the reaction paths start to diverge, suggesting the reappearance of gross hysteresis, at compositions corresponding to 'n' = 14.6 in oxidation and 'n' = 9.9 in reduction. It is more plausible (see below) that the change in c.s. plane orientation starts from, rather than ends at, an integral n value. Figure 11 shows the relation between D_{sp} and n for both (121) and (132) c.s. phases. It, together with the condition D_{sp} = constant, shows that in oxidation $n = 9$ (121) $\rightarrow$ 'n' $= 14.3_5$ (132) and, in reduction,

$$n = 16\,(132) \rightarrow \text{'}n\text{'} = 10.0_2\,(121).$$

These 'n' values are in good agreement with the observed 'n' = 14.6, 9.9; the discrepancies being only $(1.4 \pm 0.3)\%$. Of course this line of reasoning must not be pressed too far. Unless the samples are homogeneous, which seems rather unlikely, figure 3 can yield only mean values of 'n'. Nevertheless, the consistency between the observations and the hypothesis is encouraging. The fact that at least one 'n' value is non-integral will resolve itself later. Recent electron diffraction studies reveal that the structural situation is not quite as straightforward as our discussion so far has implied. But before describing these new observations we should consider further the possibilities inherent in the thermodynamic results.

† This is not quite accurate: it is the ideal D_{sp} that would be constant. The real D_{sp} is slightly greater than the ideal value by a different amount for (121) and (132) structures (Bursill & Hyde 1970); but the discrepancy is only about 2% $\equiv \sim 0.02$ nm in this region.

‡ Some $n = 10$ (121) was also present. It has $D_{sp} = 1.632$ nm; a deviation of only $+0.8\%$.

The graph of G_M^* against x^* (figure 10*a*) provides a convenient summary of the thermodynamic properties of the system. In classical terms (independent phases) it might be idealized to the schematic diagram in figure 12, in which (1) the homogeneity ranges of the phases are possibly exaggerated, (2) the G_M^* curves of some *metastable* phases have been included (e.g. (132) c.s. structures with *n odd*), and (3) we have assumed, for simplicity, that the intermediate region is from $n = 10\,(121) = \mathrm{A}$ to $n = 16\,(132) = \mathrm{B}$. We are concerned with this intermediate region $1.900 \leqslant x \leqslant 1.938$, where the equilibrium behaviour would be described by the 'common tangent' AB.

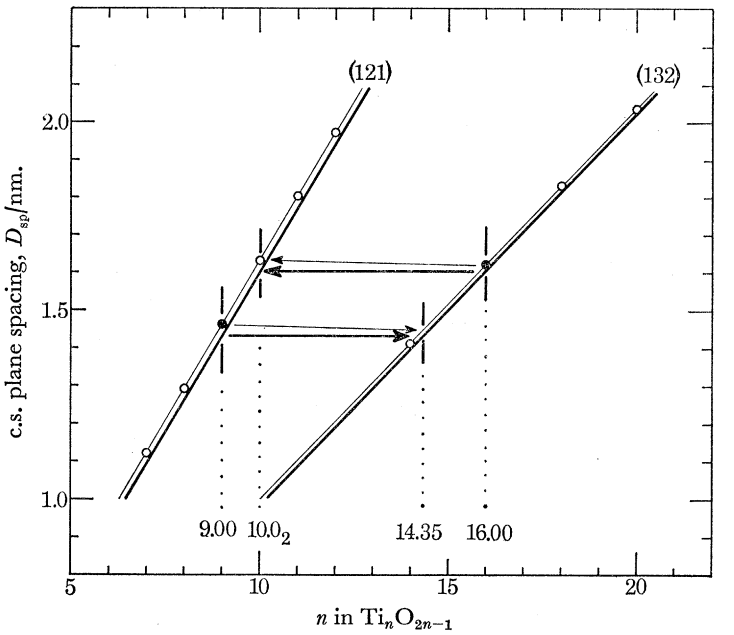

FIGURE 11. The variation of actual (thin line) and ideal (thick line) c.s. plane spacings, D_{sp}, with n in Ti_nO_{2n-1} for both (121) and (132) c.s. structures. The horizontal lines show that, at constant ideal D_{sp},

$$n = 9\ (121) \rightarrow \text{'}n\text{'} = 14.3_5\ (132)$$

in oxidation, and $n = 16\ (132) \rightarrow$ 'n' $= 10.0_2$ (121) in reduction.

Our structural knowledge suggests that along this tangent a crystal would consist of coherent domains of $n = 10$ (121) and $n = 16$ (132) c.s. structures. Thermodynamics of course, cannot tell us anything about the crystal's texture. But the next logical step is to speculate about the size of these domains. There are two extreme possibilities: *macroscopic* domains and an obviously 'diphasic' crystal with at most a few domain boundaries; and a *submicroscopic* intergrowth at about the unit cell level. In figure 13 these possibilities are depicted, schematically in *a* and *b*, and with ball models of single (100) layers in *c* and *d*.

Figure 13*c* shows that a (121) c.s. plane consists of steps, in the cation rows characteristic of rutile, of a type which we call C. Along (132) c.s. planes two types of step alternate: C and another which we call A. Note that C is in fact an A step with an extra, 'interstitial' cation. The crystal structure consists of these layers stacked with the anions in (approx.) hexagonal close-packing so that both the C and A steps line up in rows along $[1\bar{1}1]$. The first form strings of corundum type (Ti_2O_3) and the second strings of α-PbO_2 type: both in a rutile matrix. (Cf.

Bursill & Hyde 1972*b*.) Note that the c.s. planes are continuous across the boundary, which approximately bisects the angle between (121) and (132). (Cf. especially figure 13*c*†.)

In fact what we have observed is the second of the two extreme possibilities (figure 13*b*, *d*) (Bursill *et al.* 1971; Bursill & Hyde 1972*b*). Ordered intergrowths at the unit cell level produce new unit cells, and new mean c.s. planes

$$(hkl) = p'(121) + q(132),$$

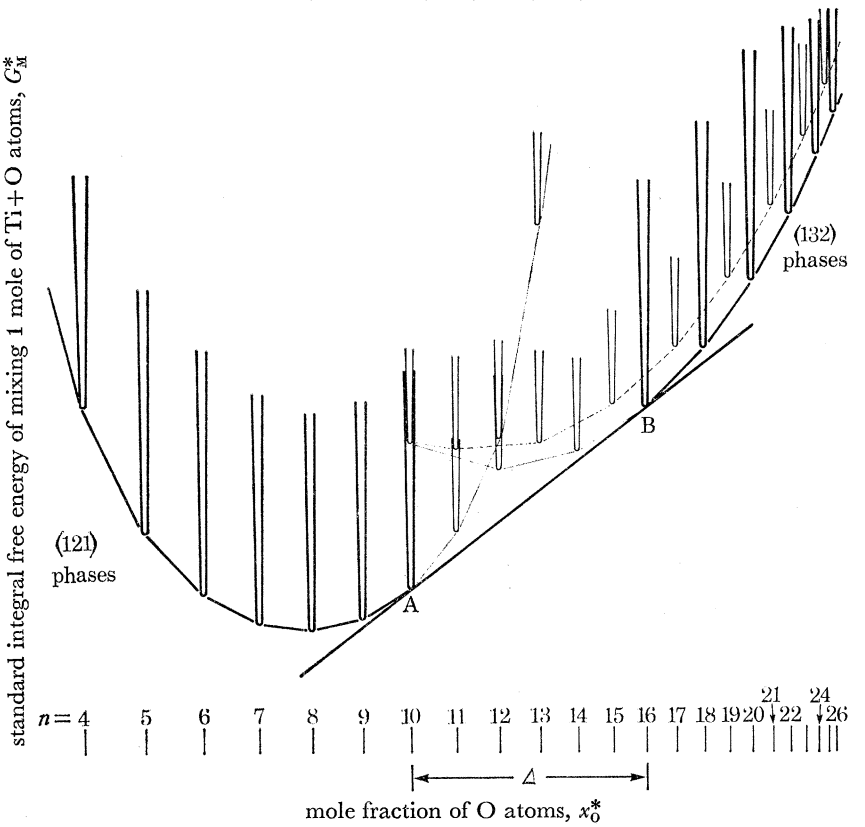

FIGURE 12. A schematic version of figure 10*a* with exaggerated homogeneity ranges for the ordered phases. The tangent AB is the equilibrium coexistence line for the highest (121) phase (with $n = 10$) and the lowest (132) phase (with $n = 16$) *if these coexist in macroscopic form in the range* Δ. The n values correspond to the stoichiometric (121) and/or (132) phases Ti_nO_{2n-1}. Some of these are metastable.

where p' and q, the proportions of the component planes in the intergrowth, are integers (one of which may be zero). Figure 13*d* shows a simple case: $p' = q = 1$ so that

$$(hkl) = (121) + (132) = (253).$$

In the intermediate region, as x decreases p'/q increases; and the c.s. planes swing from (132) towards (121) through successively higher index planes (hkl).

At every composition in the range AB (figure 12) the value of G_M^* depends on the balance struck between the energy of the (121)/(132) boundaries and the entropy of mixing the two

† In the ball-model figures the rutile-type (100) layers are not normal to $[1\bar{1}1]$. This (and the slight distortion so that the anions are in perfect hexagonal close-packing) results in the angles changing from 1.63 and 1.71 rad between the boundary and respectively (121) and (132) to 1.26 and 1.06 rad between the corresponding traces on (100).

structure types (which is not likely to be mainly configurational). The equilibrium state will be that with the lowest G_M^*. In principle it may be an intergrowth on any scale from the finest (with p' and q coprime and now representing the number of unit lengths of each type of plane in the repeat unit of the mean c.s. plane) to the coarsest (with coexisting 'grains' of the two basic c.s. structure types). What the electron microscopy/diffraction results show is that it is closer to the former than to the latter. As the composition of the crystal changes, so the proportions of (121) and (132) structures alter, and the relative widths of the (121) and (132) bands vary.† Unless the 'macroscopic mixture' of A and B is the most stable, the equilibrium G_M^* value will fall *below* the AB tangent. The slope of the real 'tangent' will then change as x changes, and so will the equilibrium value of $\Delta G_m(O_2)$.‡ This again is what is observed (figure 3).

In this composition range the intermediate c.s. planes (hkl) are reasonably well ordered in samples that have been quenched after annealing at 1300 K: the rows of diffraction spots along $\boldsymbol{g}(hkl)$ are quite sharp. But lattice images reveal that they are not as well ordered as in the related pseudo-binary system $Ti_{1-y}Cr_yO_{2-\frac{1}{2}y}$ (L. A. Bursill, to be published). We believe the binary system to be more mobile and, because the equilibrium (hkl) at a given composition is temperature-dependent, quenching is less effective in 'freezing in' the high temperature situation. 'At temperature' the TiO_x crystals may be as perfectly ordered as (Ti, Cr) O_x, with a continuous sequence of intermediate structures. On the other hand, if some disorder persists, the c.s. planes may fluctuate, in segments, about the mean direction. It is also possible that there exists an 'order–disorder' transformation between these two possibilities. The second situation provides a new mode of accommodating disorder in a crystal. *In either case we have a new method for accommodating non-stoichiometry* over a quite wide range of composition: *in the first case in a perfectly ordered way*.

All these situations are more easily visualized if we reconsider our description of an intermediate c.s. plane. It transpires that it is more convenient to take as bases the (121) c.s. plane (composed of C steps only) and the (011) antiphase boundary (APB) plane (composed of A steps only). That is, we resolve (132) = (121) + (011). Then

$$\begin{aligned}(hkl) &= p'(121) + q(132),\\ &= p'(121) + q\{(121) + (011)\},\\ &= p(121) + q(011), \text{ if } p = p' + q, \text{ and } p/q \leqslant 1;\\ &= (p,\ 2p+q,\ p+q).\end{aligned}$$

† It may be as simple as the band widths of A and B varying, but it is also conceivable that A and B may themselves change. In the latter case D_{sp}, and therefore the number of c.s. planes in the crystal, would also change. This certainly happens in the isothermal $TiO_2 + Cr_2O_3$ pseudo-binary system (Bursill *et al.* 1971; Philp, to be published), and in the TiO_x system if the temperature is varied. In the isothermal TiO_x system, with which we are concerned here, the evidence – particularly the absence of hysteresis – shows that the simpler situation obtains.

‡ For the 'macroscopic mixture' it would be independent of x, of course.

Description of plate 8

Figure 13. Coherent intergrowths of $n = 10$ (121) and $n = 16$ (132) c.s. structures in two extreme forms: macroscopic domains of each in (*a*) and (*c*); a submicroscopic intergrowth at about the unit cell level in (*b*) and (*d*). (*a*) and (*b*) are schematic diagrams with both c.s. planes, thick lines, and 'interphase boundaries', thin lines, projected edge-on (along $[1\bar{1}1]_r$). In (*b*) and (*d*) the same situations are depicted with idealized ball models of single $(100)_r$ layers: the large, light balls are oxygen atoms, slightly distorted to a regular close-packed array; the smaller, dark balls are titanium atoms.

PHILOSOPHICAL TRANSACTIONS OF THE ROYAL SOCIETY A MATHEMATICAL, PHYSICAL & ENGINEERING SCIENCES

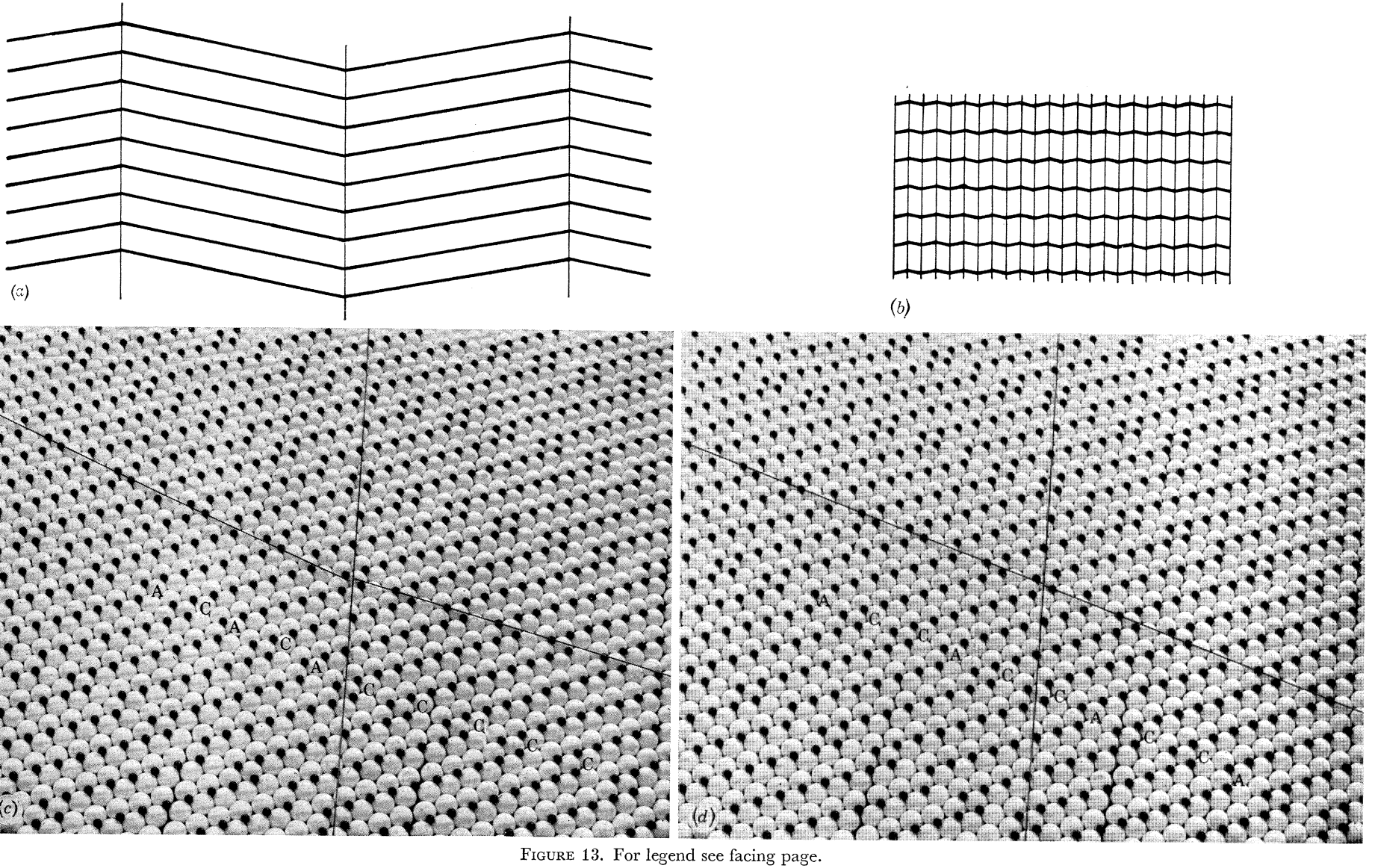

FIGURE 13. For legend see facing page.

Along an 'ordered c.s. plane' (*hkl*) the repeat unit is p C steps and q A steps. The latter do *not* change the stoichiometry; the former do, they are stoichiometric A steps each with an 'interstitial' Ti atom. The stoichiometry of an ordered (*hkl*) c.s. structure therefore depends not only on the spacing of the c.s. planes but also on their type, i.e. on the concentration of 'interstitial cations'. A change in (*hkl*) involves a variation in the proportions of A and C, i.e. in the stoichiometry of the c.s. plane. The general formula is Ti_nO_{2n-p}, where n/p is determined by D_{sp} and p by (*hkl*). (This degenerates to $Ti_{n'}O_{2n'-1}$ for $p/q = \infty$, i.e. for (*hkl*) = (121).) Along a 'disordered *mean* c.s. plane' p/q is simply the ratio of C steps to A steps, and the plane may be regarded as a disordered arrangement of 'interstitial cations' at *some* of the A steps in an APB. The relation between orientation and stoichiometry is the same as before.

Clearly, the stoichiometry of a crystal may be varied by changing the concentration of C steps on each c.s. plane without changing the number of c.s. planes. In reduction, loss of oxygen from the surface of the crystal will produce an excess of cations, which can then flow 'down' the c.s. planes, increasing p/q. Conversely, in oxidation, they flow 'up' the plane to the surface of the crystal where they combine with oxygen, and extend the crystal.

Equally clearly, they *may* ebb and flow along the plane inside the crystal so that segments oscillate (121) $\leftrightharpoons$ (132). This is the type of disorder envisaged above.

It is not an essential part of this picture of 'swinging' c.s.-planes that D_{sp} be constant or approximately so (although it *is* essential to our explanation for the absence of gross hysteresis in this region). However, it may be significant that the orientation of the (121)/(132) boundary (cf. figure 13) changes rapidly as either n value is altered. This is shown for $n = 16$ (132) and various n (121) in table 6. That the boundary should be approximately equally inclined to the c.s. planes on either side of it would seem to be a reasonable condition for a minimum interfacial energy. (This is certainly plausible for coherent 'macroscopic' grains of (121) and (132) c.s. structures, but less so for a fine intergrowth, when the concept of a 'boundary' becomes rather artificial.) A minimum interfacial energy would seem to be favourable to stability, and this clearly requires $D_{sp} \approx$ constant.

TABLE 6. COHERENT BOUNDARIES BETWEEN $n = 16$ (132) AND n (121) ORDERED C.S. STRUCTURES: D_{sp} VALUES, AND ANGLES ϕ_{121} BETWEEN BOUNDARY AND $(121)_r$ AND ϕ_{132} BETWEEN BOUNDARY AND $(132)_r$

n (121)...	4	5	6	7	8	9	10	11	12	13
D_{sp}/nm	0.62	0.79	0.95	1.12	1.29	1.46	1.63†	1.80	1.97	2.14
ϕ_{121}/rad	3.02	2.96	2.85	2.73	2.51	2.14	1.63	1.19	0.90	0.73
ϕ_{132}/rad	0.32	0.38	0.49	0.61	0.83	1.20	1.71	2.16	2.44	2.61
							↑ best fit for integral n values			

† $D_{sp} = 1.62$ nm for $n = 16$ (132).

It is possible that the suggestion of Anderson & Khan (concerning the limiting effects of lateral migration of c.s. planes) explains the minor hysteresis of 0.5 to 1.0 kJ mol^{-1} in $\Delta G_m(O_2)$ observed in this intermediate region. And our discussion earlier in this section suggests that this may result in different paths for the oxidation and reduction reactions: respectively, no c.s. planes were eliminated between $n = 9$ (121) and 'n' ≈ 14.5, or created between $n = 16$ (132) and 'n' ≈ 10. *It is now clear that there is no necessity for these* 'n' *values to correspond to* (132) *and* (121) *phases*

respectively. They may simply be the limits beyond which c.s. planes have to be destroyed or created. The c.s. planes may be simultaneously swinging and changing D_{sp}: from 'n' ≈ 14.5 to $n = 16\,(132)$ in oxidation, and from 'n' ≈ 10 to $n = 9\,(121)$ in reduction. This would bring the hypothesis and the electron microscopy and thermodynamic results into harmony in a very simple way. The 'n' values would actually be values of n/p for phases $Ti_nO_{2n-p} = Ti_{n/p}O_{2n/p-1}$.

8. A further comment on the region $1.98 \lesssim x < 2.00$

The hypothesis advanced in § 7*a* to account for the gross hysteresis in the (121) and (132) loops must also apply to the third loop which we have proposed as occupying the composition range $x \gtrsim 1.98$. Hence, one might surmise that the magnitude of the hysteresis would be similar, i.e. about $10\,kJ\,mol^{-1}$ instead of the $\sim 80\,kJ\,mol^{-1}$ that we have suggested (§ 5*d*). However, in this higher composition range the gross disorder, observed as a maze of folded c.s. planes parallel to most if not all the {132} planes, will also mean that, once it is nucleated, the longitudinal growth of a c.s. plane will be severely hampered. The faults will be 'tangled', and any significant progress towards a lower energy state will demand excessive chemical potentials or very long times.

This would also seem to be relevant to point (v) in § 4*a*.

9. Conclusion

The composition range $1.66\dot{6} \leqslant x \leqslant 2.00$ consists of five regions:

(*a*) In $1.66\dot{6} \leqslant x \leqslant 1.75$ Ti_3O_5 coexists with Ti_4O_7. The behaviour in oxidation and reduction is dominated by the difficulty of nucleating one phase in the other.

(*b*) $1.75 \leqslant x \lesssim 1.90$ is inhabited by the (121) c.s. phases. Gross hysteresis obtains and is attributed to the excess negative free energy required to nucleate new c.s. planes in order to reduce n in Ti_nO_{2n-1} and the excess free energy needed to eliminate these when n increases.

(*c*) $1.90 \lesssim x \lesssim 1.93$ is inhabited by a virtually continuous sequence of ordered or partly ordered phases in which the c.s. planes lie between (121) and (132). Composition changes are now accommodated by changing the orientation rather than the concentration of the c.s. planes. Gross hysteresis is therefore absent.

(*d*) $1.93 \lesssim x \lesssim 1.98$ is occupied by the (132) c.s. phases. Gross hysteresis again obtains, the situation being analogous to that in *b*. However, the composition intervals between adjacent ordered phases is much smaller than in *b*, and phase purity much less likely, so that phases expected to occur on crystallographic grounds are not clearly manifested.

(*e*) $1.98 \lesssim x < 2.00$. Here a subtle form of microdomain texture exists: lamellae of ordered {132} c.s. planes are dispersed in a rutile matrix. This results in a third hysteresis loop.

We are grateful for Grants AFOSR-853-65 and 67 from the Air Force Office of Scientific Research, Office of Aerospace Research of the United States Air Force, and for financial support, including a research studentship to R. R. M., from the University of Western Australia. We are indebted to Dr L. Dale of the A.A.E.C. Research Establishment, Lucas Heights (N.S.W.) who kindly performed the spectrographic analyses. Finally we would like to express our thanks to the technical staff of this department for much assistance, and to Miss Ho Kin Chee who drew some of the diagrams and Dr A. N. Bagshaw who checked some of our calculations.

PHILOSOPHICAL TRANSACTIONS OF THE ROYAL SOCIETY A MATHEMATICAL, PHYSICAL & ENGINEERING SCIENCES

References

Anderson, J. S. 1970 *Problems of nonstoichiometry* (ed. A. Rabenau), p. 1. Amsterdam: North-Holland.
Anderson, J. S. & Hyde, B. G. 1967 *J. phys. Chem. Solids* **28**, 1393.
Anderson, J. S. & Khan, A. S. 1970 *J. less-common Metals* **22**, 219.
Anderson, J. S. & Tilley, R. J. D. 1970 *J. Solid State Chem.* **2**, 472.
Andersson, S. 1960 *Acta chem. scand.* **14**, 1161.
Andersson, S., Collén, B., Kuylenstierna, U. & Magnéli, A. 1957 *Acta chem. scand.* **11**, 1641.
Andersson, S. & Jahnberg, L. 1963 *Ark. Kemi* **21**, 413.
Arnold, S., Franklin, B., Hyde, B., Lacey, N., Merritt, R. & Reece, G. 1969 *J. Phys.* E **2**, 1137.
Åsbrink, G., Åsbrink, S., Magnéli, A., Okinaka, H., Kosuge, K. & Kachi, S. 1971 *Acta chem. scand.* **25**, 3889.
Åsbrink, S. & Magnéli, A. 1959 *Acta crystallogr.* **12**, 575.
Bevan, D. J. M. & Kordis, J. 1964 *J. inorg. nucl. Chem.* **26**, 1509.
Blumenthal, R. N. & Whitmore, D. H. 1963 *J. electrochem. Soc.* **110**, 92.
Bogdanova, N. I., Pirogovskaya, G. P. & Ariya, S. M. 1963 *Russ. J. inorg. Chem.* **8**, 401.
Brauer, G. 1966 *Progr. sci. tech. rare Earths* **2**, 332.
Buerger, M. J. 1951 *Phase transformations in solids* (ed. R. Smoluchowski, J. E. Mayer and W. A. Weyl), p. 183. London: Chapman and Hall.
Bursill, L. A. & Hyde, B. G. 1970 *Proc. R. Soc. Lond.* A **320**, 147.
Bursill, L. A. & Hyde, B. G. 1971*a* *Phil. Mag.* **23**, 3.
Bursill, L. A. & Hyde, B. G. 1971*b* *Acta crystallogr.* B **27**, 210.
Bursill, L. A. & Hyde, B. G. 1972*a* *J. Solid State Chem.* **4**, 430.
Bursill, L. A. & Hyde, B. G. 1972*b* *Progr. Solid State Chem.* **7**, 177.
Bursill, L. A., Hyde, B. G. & Philp, D. K. 1971 *Phil. Mag.* **23**, 1501.
Bursill L. A., Hyde, B. G., Terasaki, O. & Watanabe, D. 1969 *Phil. Mag.* **20**, 347.
Darken, L. S. & Gurry, R. W. 1953 *Physical chemistry of metals*, chap. 10. London: McGraw-Hill.
Eikum, A. & Smallman, R. E. 1965 *Phil. Mag.* **11**, 627.
Felmlee, T. L., Hyde, B. G. & Randall, C. H. 1972 *J. Solid State Chem.* **5**, 286.
Fender, B. E. F. & Riley, F. D. 1970 *The chemistry of extended defects in non-metallic solids* (eds. L. Eyring and M. O'Keeffe), p. 55. Amsterdam: North-Holland.
Førland, K. 1964 *Acta chem. scand.* **18**, 1267.
Gilles, P. W. 1970 *The chemistry of extended defects in non-metallic solids* (eds. L. Eyring and M. O'Keeffe), p. 75. Amsterdam: North-Holland.
Golubenko, A. N. & Rezukhina, T. N. 1967 *Isvest. Akad. Nauk U.S.S.R., Neorg. Mat.* **3**, 101.
Hyde, B. G., Bevan, D. J. M. & Eyring, L. 1966 *Phil. Trans. R. Soc. Lond.* A **259**, 583.
Hyde, B. G. & Eyring, L. 1965*a* *Russ. J. inorg. Chem.* **10**, 1539.
Hyde, B. G. & Eyring, L. 1965*b* *Rare earth research* vol. **3** (ed. L. Eyring). New York: Gordon and Breach.
Iwasaki, H., Bright, N. F. H. & Rowland, J. F. 1969 *J. less-common Metals* **17**, 99.
Klinaev, V. M. & Senyavin, M. M. 1955 *Primenenie Mechenykh, Atomov v Anal. Khim., Akad. Nauk U.S.S.R., Inst. Geokhim. i Anal. Khim.*, p. 118.
Kofstad, P. 1962 *J. phys. Chem. Solids* **23**, 1579.
Kröger, F. A. 1964 *The chemistry of imperfect crystals*. Amsterdam: North-Holland.
Kubaschewski, O., Evans, E. L. & Alcock, C. B. 1967 *Metallurgical thermochemistry*, 4th edn. London: Pergamon Press.
Morozova, M. P. & Konopel'ko, M. R. 1965 *Leningrad Univ. Vestnik, Ser. Fiz. Khim.* **20**, 148.
Moser, J. B., Blumenthal, R. N. & Whitmore, D. H. 1965 *J. Am. Ceram. Soc.* **48**, 384.
Porter, V. R. 1965 Thesis, The Pennsylvania State University.
Stull, D. R. ed. 1965 *JANAF thermochemical tables*. Midland (Michigan): Dow Chemical Company.
Terasaki, O. & Watanabe, D. 1971 *Japan. J. appl. Phys.* **10**, 292.
Ubbelohde, A. R. 1956 *Br. J. appl. Phys.* **7**, 313.
Vasil'eva, I. A. & Shaulova, E. Yu. 1969 *Russ. J. Phys. Chem.* **43**, 1713.
Wadsley, A. D. 1964 *Non-stoichiometric compounds* (ed. L. Mandelcorn). London: Academic Press.
Wagman, D. D., Kilpatrick, J. E., Taylor, W. J., Pitzer, K. S. & Rossini, F. D. 1945 *J. Res. natn. Bur. Stand.* **34**, 143.
Wagner, C. & Schottky, W. 1930 *Z. phys. Chem.* B **11**, 163.
Weast, R. C. 1966 *Handbook of physics and chemistry*, 47th. edn. Cleveland: Chemical Rubber Company.
Zador, S. 1967 *Electromotive force measurements in high temperature systems* (ed. C. B. Alcock). London: Institute of Mining and Metallurgy.
Zador, S. 1969 Thesis, University of London.

PHILOSOPHICAL TRANSACTIONS OF THE ROYAL SOCIETY A MATHEMATICAL, PHYSICAL & ENGINEERING SCIENCES

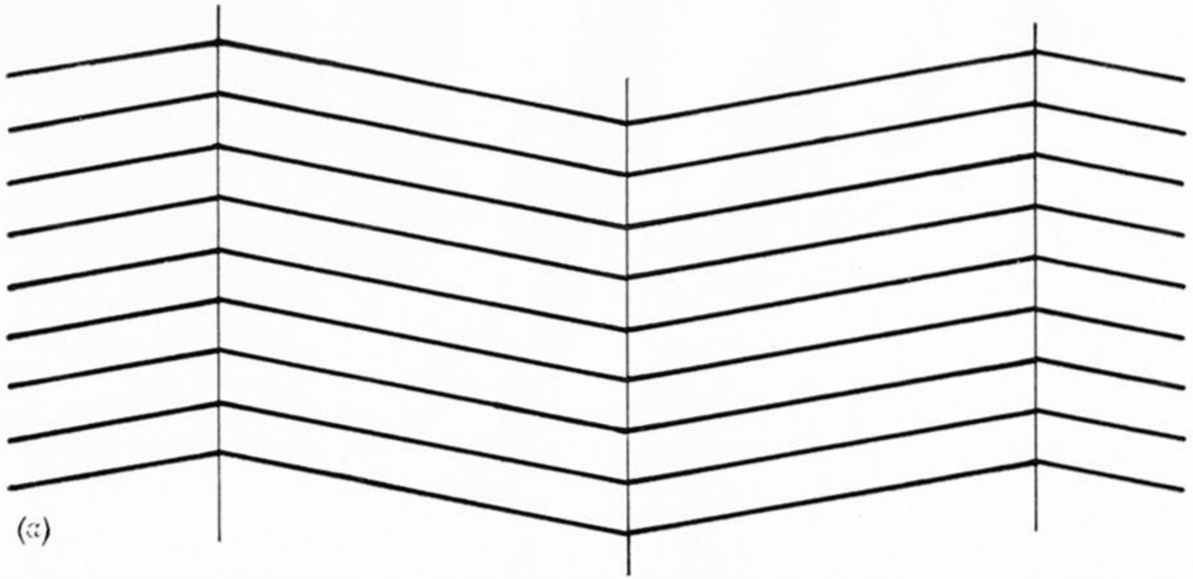

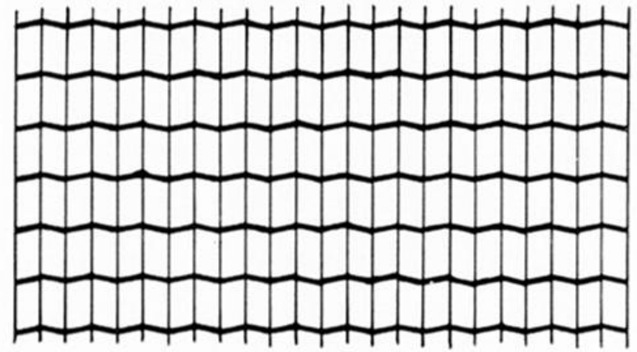

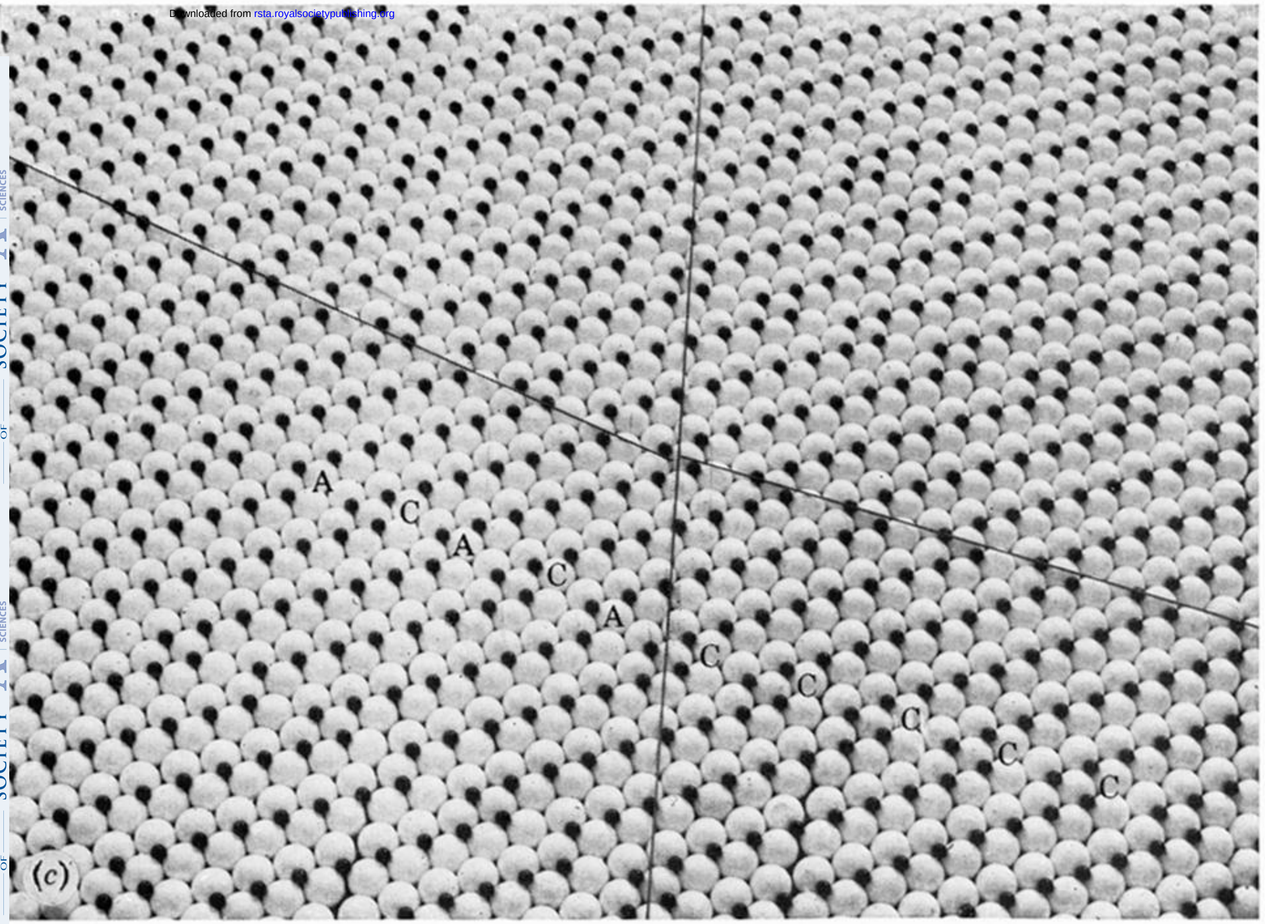

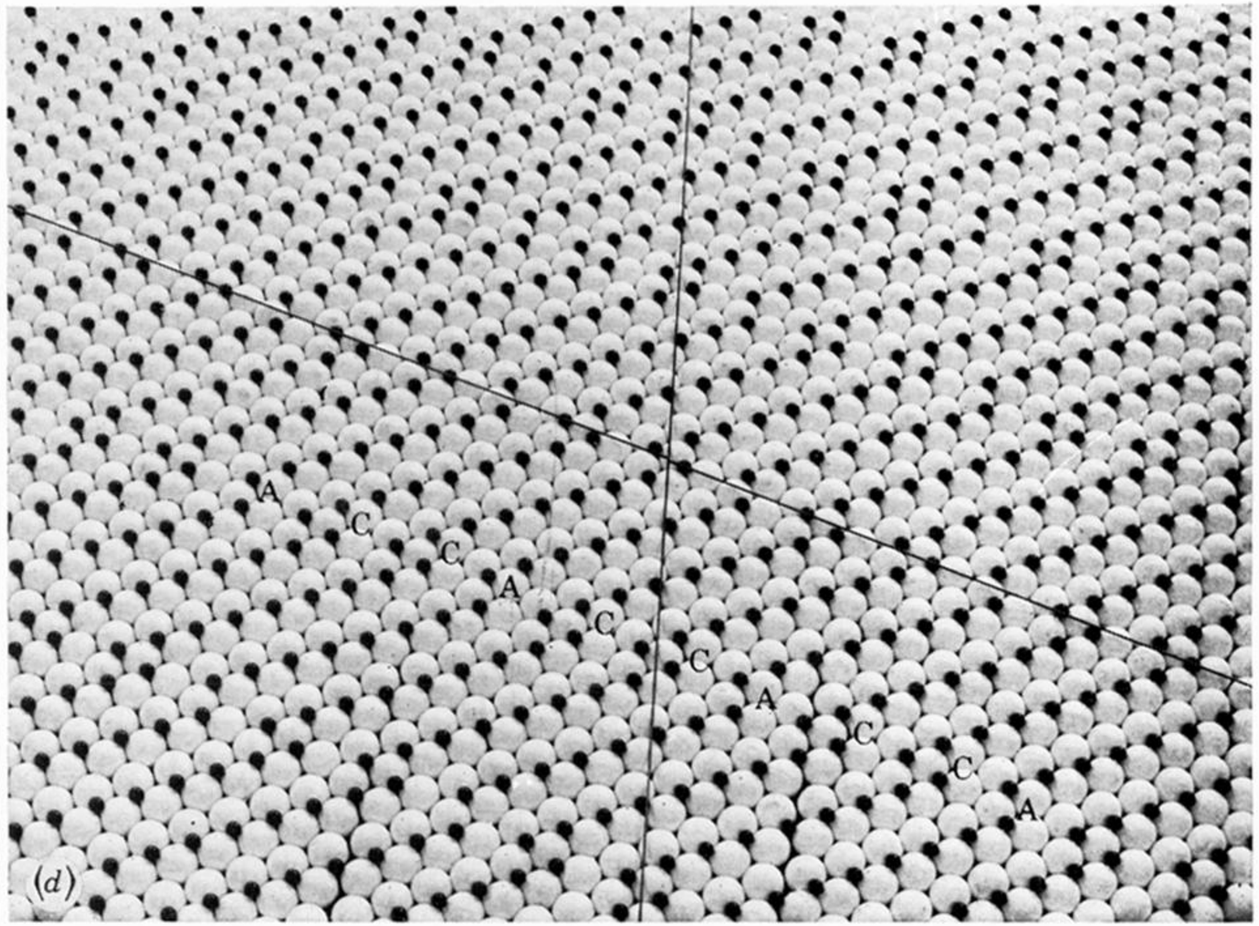

FIGURE 13. For legend see facing page.